FABRICATION AND CHARACTERIZATION OF SILK SERICIN BASED COMPOSITE FILMS FOR BIOMEDICAL APPLICATIONS

A THESIS SUBMITTED TO
THE GRADUATE SCHOOL OF NATURAL AND APPLIED SCIENCES
OF
MIDDLE EAST TECHNICAL UNIVERSITY

BY

ALPER HALİLOĞLU

IN PARTIAL FULFILLMENT OF THE REQUIREMENTS
FOR
THE DEGREE OF MASTER OF SCIENCE
IN
METALLURGICAL AND MATERIALS ENGINEERING

JANUARY 2023

Approval of the thesis:

FABRICATION AND CHARACTERIZATION OF SILK SERICIN BASED COMPOSITE FILMS FOR BIOMEDICAL APPLICATIONS

submitted by **ALPER HALİLOĞLU** in partial fulfillment of the requirements for the degree of **Master of Science** i**n Metallurgical and Materials Engineering, Middle East Technical University** by,

Prof. Dr. Halil Kalıpçılar
Dean, Graduate School of **Natural and Applied Sciences** _____

Prof. Dr. Ali Kalkanlı
Head of the Department, **Metallurgical and Materials Engineering** _____

Assoc. Prof. Dr. Batur Ercan
Supervisor, **Metallurgical and Materials Engineering, METU** _____

Examining Committee Members:

Prof. Dr. Abdullah Öztürk
Metallurgical and Materials Engineering, METU _____

Assoc. Prof. Dr. Batur Ercan
Metallurgical and Materials Engineering, METU _____

Prof. Dr. Cevdet Kaynak
Metallurgical and Materials Engineering, METU _____

Assist. Prof. Dr. Yusuf Keleştemur
Metallurgical and Materials Engineering, METU _____

Assoc. Prof. Dr. Sedat Odabaş
Chemistry, Ankara University _____

Date: 18.01.2023

I hereby declare that all information in this document has been obtained and presented in accordance with academic rules and ethical conduct. I also declare that, as required by these rules and conduct, I have fully cited and referenced all material and results that are not original to this work.

Name Last name : Alper Haliloğlu

Signature :

ABSTRACT

FABRICATION AND CHARACTERIZATION OF SILK SERICIN BASED COMPOSITE FILMS FOR BIOMEDICAL APPLICATIONS

Haliloğlu, Alper
Master of Science, Metallurgical and Materials Engineering
Supervisor: Assoc. Prof. Dr. Batur Ercan

January 2023, 66 pages

Silk Sericin (SS) is one of the two major proteins in silk fiber and it is discarded as a waste in the silk industry. Recently, sericin captured attention in the biomedical field due to its variable amino acid composition and diverse functional groups. The physical and chemical properties of silk sericin can be adjusted via incorporation of different secondary phase additives for biomedical applications. However, brittle nature, low mechanical properties, and inability to avoid bacterial growth by itself limits its use in such areas. In this study, high temperature and pressure method is used to extract sericin from silk cocoons. To fabricate sericin based composite films, extracted sericin is combined with different agents, namely glycerol to overcome the brittle characteristics, as well as Sr and Zn incorporated bioactive glass (BG) particles and graphene oxide (GO) to provide mechanical durability and antibacterial properties. SEM images of the sericin based composite films showed that reinforcements were homogenously distributed throughout the films without any agglomeration. Thermogravimetric analysis showed that nearly 35% of the initial mass of the sericin films were lost during the early stages of degradation, which was correlated with glycerol diffusing out the system. Moreover, approximately 85-105 % swelling was observed upon soaking sericin films in

1xPBS, which indicated their good water retention ability. The Young's modulus values of silk sericin based films increased from 16.7±0.9 MPa up to 19.3±1.9 MPa and 22.4±0.6 MPa upon 1% GO and 7% BG addition, respectively. When L929 fibroblast cells were treated with extracts of silk sericin films, no toxicity was observed and cellular viability was promoted up to 7 days of culture *in vitro*. Both reinforcement materials (GO and BG) exhibited antibacterial activity against gram-positive *Staphylococcus aureus* (*S. aureus*) and gram-negative *Escherichia coli* (*E. coli*) strains in a concentration dependent manner. Cumulatively, the obtained results showed that silk sericin based composite films are promising candidates for biomaterial applications.

Keywords: Silk Sericin, Composite Film, Bioactivity, Antibacterial, Natural Polymer

ÖZ

BİYOMEDİKAL UYGULAMALAR İÇİN SERİSİN BAZLI KOMPOZİT FİLMLERİN ÜRETİMİ VE KARAKTERİZASYONU

Haliloğlu, Alper
Yüksek Lisans, Metalurji ve Malzeme Mühendisliği
Tez Yöneticisi: Assoc. Prof. Dr. Batur Ercan

Ocak 2023, 66 sayfa

İpek Serisin (SS), ipeği oluşturan iki ana proteinden biridir ancak ipek endüstrisinde genellikle atık olarak görülmektedir. Serisin son zamanlarda, çeşitli fonksiyonel grupları ve değişken amino asit bileşimi nedeniyle biyomedikal alanda ilgi görmeye başlamıştır. Serisinin fiziksel ve kimyasal özellikleri, farklı ajanların dahil edilmesiyle biyomedikal uygulamalar için ayarlanabilir. Ancak kırılganlığı, düşük mekanik özellikleri ve bakteri büyümesini kendi başına engellemede yetersiz kalışı bu tür alanlarda kullanımını kısıtlamaktadır. Bu çalışmada serisin ipek kozasından yüksek sıcaklık ve basınç yöntemi kullanılarak ayrılmıştır. Elde edilen serisin kompozit filmler üretmek amacıyla çeşitli ajanlarla birleştirilmiştir. Bu ajanlardan gliserol serisinin kırılganlık sorunu çözmek amacıyla plastikleştirici olarak kullanılırken mekanik dayanımı ve antibakteriyel özelliklerini geliştirmek için grafen oksit (GO) ve Sr ve Zn katkılı biyoaktif cam (BG) ile kombine edilmiştir. Serisin bazlı filmlerin SEM görüntüleri takviye parçacıkların topaklanma olmadan homojen bir şekilde dağıldığını göstermiştir. Filmlerin degradasyonun erken aşamalarında sistemden ayrılan gliserol sebebiyle ağırlıkalrının yaklaşık %35ini kaybettikleri ortaya konulmuştur. Filmlerin 1xPBS içerisinde yaklaşık %85-105 şişme göstermesi iyi bir su tutma özellikleri olduğunu

gösterir. Ek olarak, serisin bazlı filmlerin Young's modülüsleri 16.7±0.9 MPa değerinden %1 GO ve %7 BG eklenen filmlerde sırasıyla 19.25±1.9 MPa ve 22.4±0.6 MPa seviyelerine kadar çıktığı görülmüştür. Ayrıca, serisin film ekstraktlarının L929 fibroblast hücreleri ile etkileşimlerinde bir toksisite göstermedikleri, hücrelerin 7 güne kadar başarılı bir şekilde canlılıklarını koruyup çoğaldıkları *in vitro* hücre kültürü testlerinde görülmüştür. Her iki katkı malzemesinin de (GO ve BG) gram pozitif *Staphylococcus aureus* (*S. aureus*) ve gram negative *Escherichia coli* (*E. coli*) bakterilere karşı kompozisyona bağlı olarak antibakteriyel etki gösterdiği gözlemlenmiştir. Sonuç olarak ipek serisin bazlı kompozit filmlerin biyomedikal uygulamalar için gelecek vadeden adaylar olduğu görülmüştür.

Anahtar Kelimeler: İpek Serisin, Kompozit Film, Biyoaktivite, Antibakteriyel, Doğal Polimer

To my beloved family…

ACKNOWLEDGMENTS

I wish to express my deepest gratitude to my supervisor Assoc. Prof. Dr. Batur Ercan who gave me the unique opportunity to work in his research group with remarkable people. His approach to research, guidance and vision enlightened me about academy and helped me to design my future career. His criticism, motivation and dynamism always inspired and encouraged me to keep going. It was a great honor and privilege to study under his counseling.

I would also like to thank Cansu Taşar for all the support and patience throughout my experiments. Also, Yiğithan Tufan for his guidance in data collection and analysis. With their help, I could achieve more than I imagined.

I'd also like to thank all my laboratory mates, particularly Yağmur Göçtü and Melisa Kafalı for their sincere friendship and assistance. Your positivism makes everything easier especially before the stressful deadlines. I will always consider myself lucky to know you and never forget all the fun times through those years.

I thank the members of Metallurgical and Material Engineering Department and Central Laboratory of Middle East Technical University, notably Nilüfer Özel for her help in XRD and Serkan Yılmaz for his help in SEM.

Finally, I'd like to thank my family: my parents Ayşegül & Engin Haliloğlu for their love, support, caring and patience. They would always be there for me for my whole life. In addition, I have special thanks to my sister İzel Haliloğlu who always entertains and inspires me with her idiosyncratic ways of thinking. She was my main motivation source during the hardest times of these thesis studies.

TABLE OF CONTENTS

LIST OF TABLES

TABLES

LIST OF FIGURES

FIGURES

LIST OF ABBREVIATIONS

ABBREVIATIONS

SS: Silk Sericin

GO: Graphene Oxide

BG: Sr and Zn doped Bioactive Glass

SSG: Sericin + 50% Glycerol film

SSGD: Sericin + 50% Glycerol film soaked in 1xPBS for 72 h.

SSG-xGO: Sericin + 50% Glycerol + x% GO films

SSG-xGOD: Sericin + 50% Glycerol + x% GO films soaked in 1xPBS for 72 h.

SSG-xBG: Sericin + 50% Glycerol + x% BG films

SSG-xBGD: Sericin + 50% Glycerol + x% BG films soaked in 1xPBS for 72 h.

SF: Silk Fibroin

rpm: Revolution per minute

SEM: Scanning electron microscopy

TEM: Transmission electron microscopy

XRD: X-ray diffraction

FTIR: Fourier transform infrared spectroscopy

TGA: Thermal gravimetric analysis

PBS: Phosphate buffer saline

DMEM: Dulbecco’s Modified Eagle Medium

FBS: Fetal bovine serum

MTT: 3- (4,5-dimethyl-2-thiazolyl)-2,5-diphenyl-2H-tetrazolium bromide

DMSO: Dimethyl sulfoxide

TSB: Tryptic soy broth

S. aureus: *Staphylococcus aureus*

P. aeruginosa: *Pseudomonas aeruginosa*

LIST OF SYMBOLS

SYMBOLS

nm: nanometer

μm: micrometer

θ: Theta

h: hours

CHAPTER 1

INTRODUCTION

1.1 Silk Sericin

Sericin is one of the two main proteins which forms the *bombyx mori* silkworm silk. Cocoons are formed by two fibroin fibers glued by sericin, as shown in Figure 1.1 [1]. Although fibroin is vastly used in silk industry, sericin was treated as a waste product and removed from fibroin to improve its performance [2]. Also, for decades, it was believed that sericin caused allergic reactions, inflammation-inducing effects, and immunogenicity [3]. Recently, with enhancing number of studies claiming otherwise [3-5], this natural polymer gained attraction in the biomedical field due to its unique properties, such as biocompatibility, biodegradability, water retention, and gas permeability, [6, 7]. However, nearly 50.000 tons of sericin is still discarded in the textile wastewaters each year [7, 8], which can be potentially be recycled and used in various biomedical applications.

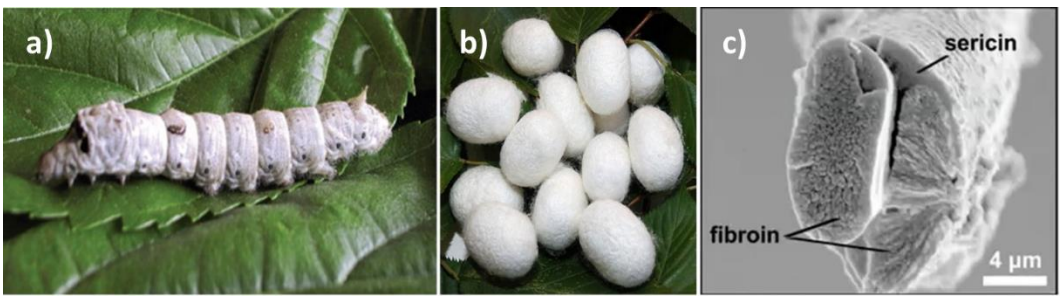

Figure 1.1 a) *Bombyx mori* silkworm, b) *Bombyx mori* silkworm cocoons and c) cross-sectional SEM image of raw silk [9, 10].

According to water solubility and polarity of its amino acids, sericin can be divided to three layers where the content of polar amino acids is decreased through inner layers. Thus, the inner layer requires acid treatment for extraction, whereas the outer layers can easily be removed from fibroin with boiling or dissolving in water by heat and pressure [11]. Sericin can be used as several forms, including films, sponges or fibers depending on the production method [6, 7]. Independent of its form, sericin is highly brittle and cannot inhibit bacterial growth sufficiently by itself. These aspects should be improved to be utilize sericin in biomedical applications.

1.2 Structure of Silk Sericin

Sericin has a molecular weight range of 24 to 400 kDa. It is a hot water-soluble globular protein which forms 25-30% of the silk fiber [1, 6, 7, 11]. It consists of 18 types of amino acids, among which serine, aspartic acid and glycine are the most abundant amino acids [7, 11], as seen in Figure 1.2. Majority of the amino acids in sericin are polar containing hydroxyl, carboxyl, or amino groups; only 22% of them are non-polar [11]. Hydrophilic ones (especially serine and aspartic acid) are responsible for the water solubility of sericin.

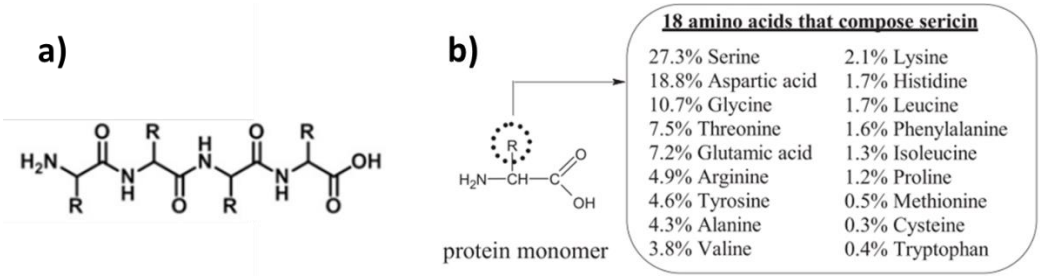

Figure 1.2 a) Molecular chain and b) amino acid composition of sericin [12].

Secondary structures were formed by folding of polypeptides via hydrogen bonding between amine and carboxyl groups of the amino acids. α-helices and β-sheets were the most commonly occurring secondary structures. Unfolded regions

are described as random coils and regions where polypeptides change folding direction is called β-turns [13]. Depending on the extraction process, secondary structure content of sericin can be varied, as shown in Table 1.1. Nevertheless, when extracted via the high temperature and pressure (HTHP) method, the conformation of sericin mostly contains random coils and β-sheets, which are responsible for amorphous and crystalline regions, respectively [1, 11]. Although weaker than covalent bonds, the hydrogen bonds in β-sheets were mainly responsible for the mechanical properties of the sericin.

Table 1.1 The effect of extraction method on secondary structure of sericin [14].

Extraction Method	Secondary Structure (%)			
	α-Helix	β-Sheet	Turns	Random Coils
Conventional	28.8	0.0	35.1	36.1
Heat (boiling in water)	0.0	56.2	2.5	41.3
Urea-degradation	2.8	54.5	4.0	38.7
Alkali-degradation	28.5	0.0	33.8	37.8
Acid-degradation	14.9	34.8	17.0	33.3

Silk sericin (SS) can be extracted from silk yarn by physical, chemical or biological methods, as listed in Table 1.2 [14]. Each method has different advantages and drawbacks. In silk industry, soaps, detergents and sodium bicarbonate solution were conventionally used to separate sericin from fibroin. However, these treatments highly degrade sericin and it is extremely difficult to remove detergents from the remaining sericin [14]. Although not all sericin can be separated, high temperature and pressure (HTHP) extraction was frequently used in experimental studies. Moreover, it does not require time consuming purification steps and higher MW sericin can be obtained with hot water treatment [7, 11]. In addition, it was shown that SS extracted via heat promote viability of L929 fibroblast cells better than other alternative extraction processes [15].

Table 1.2 Extraction methods of silk sericin [14].

		Name of methods	Degumming conditions	Yields (%)
Degumming methods	Physical	Electrolyzed H_2O	≥pH 11.50; 100 °C; 1:40 (W/V); 20 min 2	~27
		HTHP H_2O	~120 °C; 1:25 (W/V); 60 min	~15
		Infrared heating H_2O	120 °C; pH 6.80; 1:20 (W/V); 60 min	~26
		Ultrasound wave	pH 8.0–9.0; 60 °C; 1:30 (W/V); 90 min	~21
	Chemical	Na_2CO_3	0.1–0.5%, pH 11.0; 100 °C; >20 min	~30
		pH-adjusted LiBr	9 M LiBr; pH 5.0–7.0	·
		Urea buffer	8 M, pH 7.0; 80–90 °C; 120 min, >2 times	~27
		Neutral soaps	25%, pH 7.0.; 93 °C; 1:30 (W/V); 30 min 3	~20
		Acidic solution	pH 2.0.; 100 °C; 1:18 (W/V); 30 min	~27
	Biol	Microbial	pH 7.0.; 28 °C; 1:30 (W/V); 30 min	
		Protease	pH 10.0.; 37 °C; 1:30 (W/V); 180 min	~20
Recycling methods	Physical	Film filtration	Micro- and nano-filtration, room temperature	>90
		Electrolysis	25 V_{DC}; 40–60 min	20–75
		Freezing–thawing	−20–30 °C; 5 h 2	>80
	Chemical	pI-centrifuge	~pH 8.0; 0.1% HACC	76
		Coagulation	pH 8.0.; 75 °C; 1:30 (W/V); 480 min; 1 time	95
		Denaturation in solvents	90% (v/v) ethanol	>90

Extraction method, concentration and processing parameters are directly affecting final characteristics of the sericin, such as MW and crystallinity, and therefore they have a strong influence on final performance of sericin [6, 7, 11]. Sericin shows thermo-reversible sol-gel transition due to its hydrogen bonds. That is, when temperature is above 70-80 °C, it stays in the solution form, however when the temperature is decreased it quickly becomes gel [16]. That said, exposure to heat can cause degradation at longer times and results in lower MW. As the MW increased (due to concentration or low extraction times), its gelation time, gel strength, crystallinity, mechanical and thermal properties also increase, while porosity and swelling ratio decreased [16, 17]. Moreover, it was observed that MW has no or very small influence on the cytocompatibility of sericin [16]. Recently, advanced extraction methods were developed using ultrasound or infrared heating, yet they need extra equipment, and thus increase the cost of extraction [14].

1.2.1 Comparison of Sericin and Fibroin

Silk fibroin (SF) consists of heavy and light polypeptide chains. Although containing similar amino acids with SS, their amounts and sequences in SF is

highly different than sericin [13]. Glycine and alanine form the majority of SF heavy chain and form large hydrophobic domains [18]. Moreover, β-sheet formation in SF is induced mainly due to the specific sequence of these two amino acids [19]. As a result, SF became more hydrophobic and easier to form β-sheet crystallites than sericin which is responsible for its slower degradation rate and superior mechanical properties. In spite of its inferior mechanical properties, hydrophilic sericin shows better chemical and biological activity [20-22]. Hydroxyl, carboxyl, and amino groups in sericin facilitates it to easily form composites with different reagents. The aforementioned advantages of sericin are used in various publications to solution issues regarding its brittle characteristics. Blending with other synthetic polymers like poly(vinyl alcohol) (PVA), chitosan or polymethyl methacrylate (PMMA) [23-26], using cross-linkers such as poly(ethylene glycol) diglycidyl ether (PEG-DE), glutaraldehyde or dimethylurea (DMU) [27], and dissolving in various solvents are proposed in the literature. However, most of these chemicals are toxic and lower biocompatibility of sericin. Alternatively, the use of plasticizers is a promising approach to solve this brittleness issue of sericin.

1.2.2 Glycerol as Plasticizer

Among many plasticizers, such as ethylene glycol or sorbitol, glycerol ($C_3H_8O_3$) is the most commonly used and effective one to enhance flexibility of polymers [28] due to its compatibility with polymers, easy penetration, and non-volatile nature [29]. Main plasticizing mechanism of glycerol can be explained with gel and free volume theories. According to this theory, smaller glycerol molecules can easily enter the sericin polymer chains, which replaces the intramolecular hydrogen bond network by forming hydrogen bonds between sericin and glycerol. During that process compact structure of sericin is changed by the increase of free volume, especially in the random coil regions. Thus, chain mobility gets easier, and plasticity is increased [28, 29]. Moreover, glycerol has been used in skincare

products due to its water absorption ability which reinforces skin barrier by preventing water loss. In fact, it can penetrate the stratum corneum layer of the skin without disrupting its structure and helps hydration [30], which could also be a desired property for wound dressing applications. In addition to hydration, glycerol shows anti-irritant and even wound healing effects [30, 31].

CHAPTER 2

LITERATURE REVIEW

2.1 Sericin Based Biomaterials

In the market, pure sericin and sericin powders were produced by some companies including Silk Biochemical Co., Huzhou Longs Biochem Co., Xian Tianyi Biotechnology Co., Shaanxi Seyon Industry Co., (China) and Wako (USA). Apart from these companies, sericin containing products were produced for cosmetics, hair care, food, and fabric industries by various companies, such as Acca Kappa, Comfort Zone (Italy), Aurora Silk, The Hair Care Company, Better for Babies, Plank (USA), SINOSILK, Nanjing Valued Textile Co. (China), Elmiplant Romania (Romania), Dr. Temt (Austria) and Seiren Co., Toyota (Japan) [6]. Due to having desirable and controllable properties, sericin attracted attention in biomedical applications and investigated for several forms such as films, scaffolds or hydrogels, as shown in Figure 2.1 [6, 7].

Among the potential uses of sericin, sericin based films are generally investigated for skin and bone tissue engineering applications. Due to its inherent properties sericin based dressings are suitable for skin regeneration and wound healing [7]. Also, they were shown to promote bone regeneration when wrapped on the metallic implant surfaces by enhancing adhesion and proliferation of osteoblasts [32].

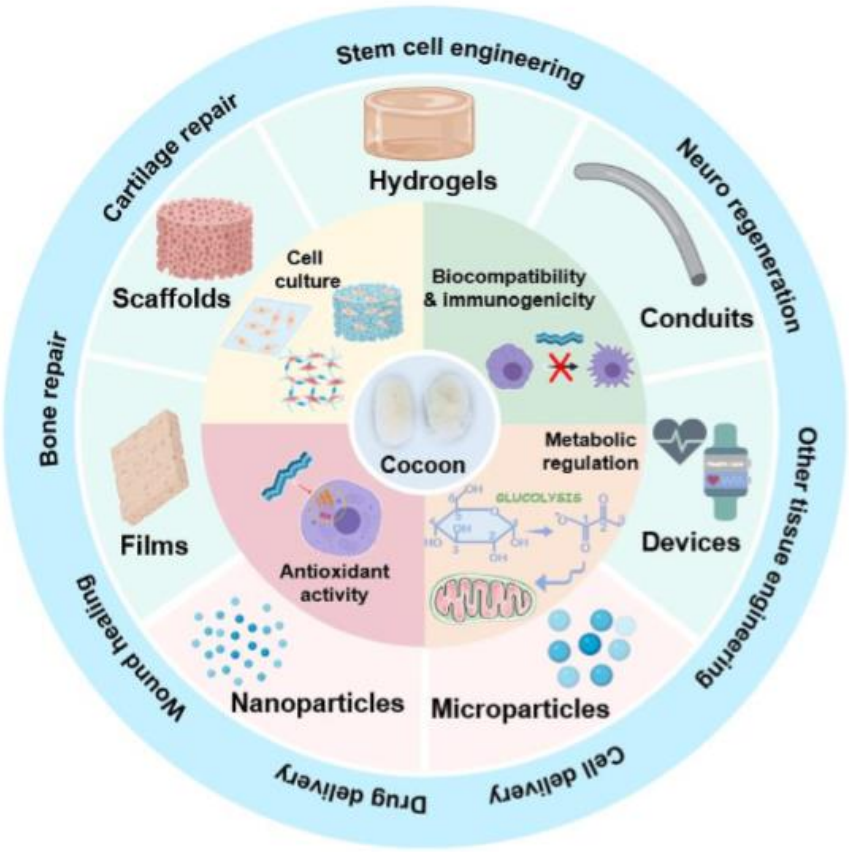

Figure 2.1 Forms and application areas of silk sericin based materials [7].

2.2 Glycerol and Sericin

In literature, the effect of glycerol on sericin was investigated in a couple of studies. As a plasticizer, while increasing the flexibility and elongation, addition of glycerol induces β-sheet formation in the secondary structure of sericin. This phenomenon was observed as a shift in amide I peak of FTIR spectra to β-sheet region and supported with XRD results, where peak intensities increased with increasing glycerol content [27-29]. Zhang et. al. explained this effect with increasing both β-sheet and random coil structures simultaneously with an associated decrease in β-turns up to 40% glycerol incorporation. [27]. Contrary to Zhang et al., Yun et. al. proposed that the amount of random coils also decreased

with addition of glycerol. Because of an increase in the moisture content due to the hygroscopic nature of glycerol, glycerol and water show synergistic effect in improveing plasticity after 50% glycerol concentration [28]. In both studies, it was observed that % elongation of the sericin films increased, while elastic modulus and tensile strength decreased after 20% glycerol addition. Up to the 20% glycerol addition, slight increase in the mechanical properties were observed due to physical interactions between glycerol, sericin and water molecules [27]. However, effective plasticization was achieved after 50% glycerol concentration [28].

2.3 Nanoparticles

Aside from plasticizers, another way to alter final properties of sericin is making composite structures by using reinforcement materials like nanoparticles, nanosheets, nanofibers etc. In addition to increasing mechanical properties, extra biological properties could be provided to the system via reinforcements such as bone forming ability and anti-bacterial properties or angiogenesis.

2.3.1 Graphene Oxide for SS-GO Films

Due to its functional groups, GO can easily and stably dispersed in water compared to other carbon derivatives [33]. Thanks to effective dispersion, it can be a good alternative for composite film applications. Aside from easy processing and large scale production, antibacterial activity of GO makes it a desirable nanomaterial for biomedical applications [33-37]. Antibacterial mechanism of GO is generally explained with direct contact and reactive oxygen species (ROS) formation mechanisms [33, 34]. In direct contact mechanism, small and sharp GO sheets with functional groups easily interact with bacterial cells, which disrupts and damages cell membranes, and consequently kills them [34, 38]. GO could show superoxide independent oxidative stress on bacterial cells through generation of hydroxyl

radicals [35]. For the case of mammalian cells, GO shows only a mild cytotoxicity at low doses [34].

Due to its nano size, small amounts of GO can alter the properties of sericin significantly. In literature there is a couple studies which used sericin and GO together. Yun et. al. used GO and made SS/Glc/GO nanocomposite films. Due to the strong interfacial interactions between SS and GO tensile strength and Young's modulus of final films was increased up to 15 and 600 MPa, respectively, while the crystallinity of the films decreases. Yet, due to the glycerol content crystallinity was balanced and elongation at brake showed an increase up to 40% [29]. On the other hand, Qi et. al. fabricated SerMA/GO hydrogel (SMH/GO) and showed that in addition to increasing mechanical properties, SMH/GO hydrogels facilitate osteogenesis by regulating autologous BMS migration and osteogenic differentiation [39]. Jayavardhini *et al.* found that GO impregnated sericin/collagen scaffolds showed blood compatibility, while demonstrating new blood vessels formation [40]. Recently, Zhang et. al. proposed chitosan/sericin/Ag@MOF–GO composite system as an antibacterial wound dressing alternative [41].

2.3.2 Bioactive Glasses for SS-BG Films

Bioactive glasses could be a good alternative for sericin based composite films for biomedical applications since they are already biocompatible and easily doped with additional ions which gives them the desired biological properties [42]. Dopant elements like Cu or Sr can increase the bone forming ability of the sericin films [43, 44]. Recently, it is observed that Sr improves the formation of blood vessel tissue [45], while Ag or Zn doping could increase the antibacterial activity of sericin with the release of positively charged ions as well as direct contact mechanisms [46, 47]. With the combination of more than one doping element into bioactive glass reinforcement, various biological properties can be provided to sericin. Although not investigated with, there are various examples which use bioactive glass with fibroin especially for its osteogenic properties. Christakiran et.

al. used electrospinning to make fibroin/bioactive glass composite mats which could support the growth and maturation of osteogenic and chondrogenic cells. While Zhu et. al. formed a SF/BG bioactive film, which showed enhanced proliferation of osteoblasts compared to SF films [48]. Moreover, it was reported that, Sr doped BG promotes early angiogenesis [44, 45] which is a crucial property for wound dressings. Due to the aforementioned biological advantages, along with tunable nature of doping element incorporation, using bioactive glass with sericin could be a promising topic.

2.4 Wound Dressings

Accute wounds can be described as the defects in epidermis/dermis of the skin layer which can heal naturally [49]. However, this healing process can take a long time. It was known that with the help of temporary wound dressings, healing duration can be reduced by facilitating healing steps [50]. Different types of wound dressings were used to improve wound healing process [51]. However, due to the challenging nature of the healing process, the search for an ideal wound dressing system still continues [52].

Wound healing occurs in four stages [53, 54]. First stage is haemostasis where blood vessels tightened to minimize bleeding and form blood cloth. During this process, fibrin protein forms cross-links at the wound area to prevent bleeding and any contaminants to enter from the wound area. Afterwards, iflammation phase starts. Due to histamine release from the damaged tissue, blood vessels are expanded, called vasodilation, which facilitates migration of white blood cells (macrophages) to the wound site to fight bacteria via phagocytosis. After 2 to 4 days, proliferation stage begins where fibroblast cells entered the wound area and synthesize collagen which replaces the fibrin. Fibroblasts trigger endothelial cells to prolifereate, epidermis reforms and dermis contracts to close the wound. Final stage is remodeling and maturation phase where scab slabs off and collagens

rearranges which cause denser tissue. fibroblasts were reduced. As a result, a scar tissue is formed via fibrosis [51]. This prosess shematically shown in Figure 2.2.

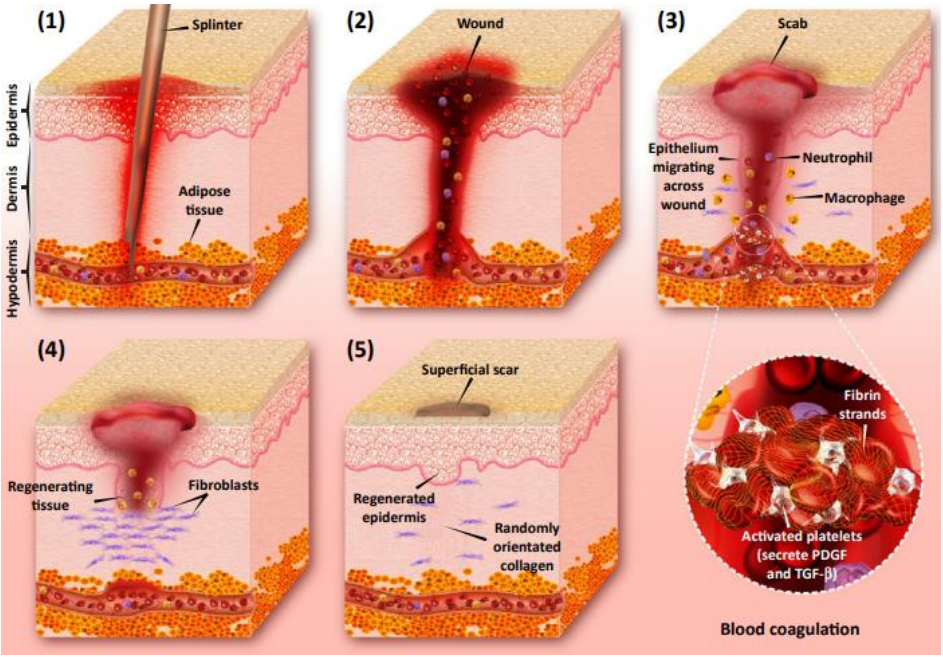

Figure 2.2 Schematic representation of different stages in the wound healing process [54].

Wound dressings should provide a convenient environment to facilitate the healing process in the wound area. Therefore, dressing material should be selected considering their ability to maintain/provide moisture, allow gas exchange between environment and wound area, facilitate epidermal migration, avoid bacterial growth, maintain sufficient temperature as well as promoting angiogenesis and connective tissue synthesis [49, 52, 53]. Moreover, they should not be toxic or allergenic. Various materials were used as wound dressings throughout centuries [55]. Although traditional dressings, which made of cotton fibers, polyesters or rayon have still been used in some applications due to their accessibility and affordability, modern dressings are fabricated to overcome their drawbacks, such as drainage or changing frequency. Nowadays, more and more alternative dressings

emerge in the form of films, foams, hydrogels, hydrocolloids, even tissue engineered skin substitutes [53, 56]. Some of the commercially available products and their characteristics are listed in Table 2.1.

Table 2.1 Examples for the commercially available wound dressing products [53].

Type of dressing	Commercially available products	Notes
Gauze	Curity, Vaseline Gauze, Xeroform	Inexpensive, drying, may cause further injury on changing
Films	Bioclusive, Blisterfilm, Cutifilm, Flexigrid, OpSite, Tegaderm	Occlusive, retains moisture, only for non-exudative wounds
Hydrocolloids	Aquacel, Comfeel, DuoDERM, Granuflex, Tegasorb	Long times between changes, fluid-trapping, occlusive, not for infected wounds
Hydrogels	Carrasyn, Curagel, Nu-Gel, Purilon, Restore, SAF-gel, XCell	Rehydrates dry wounds, easy removal/ changes, may cause over-hydration
Foams	3M Adhesive Foam, Allevyn, Lyofoam, Tielle	Moderately absorbent, insulating
Alginates	Algisite, Kaltostat, Sorbsan, Tegagen	Highly absorbent, hemostatic
Hydrofibers	Aquacel Hydrofiber	Highly absorbent
Tissue engineered skin substitutes	Alloderm, Apligraf, Biobrane, Bioseed, Dermagraft, Epicel, EZ Derm, Hyalograft, Integra Omnigraft, Laserskin, Myskin, TransCyte	Addresses deficient growth factors and cytokines, expensive, risk of infection, antigenicity

Most of the commercial dressing products are made of synthetic polymers. Majority of them are be considered as inactive, which only act as a barrier between wound tissue and its environment. Although they have some advantages, nowadays more natural polymers alternatives are investigated as a replacement for these synthetic dressings due to environmental and biological concerns [51, 55]. Among them, collagen, alginate, chitosan, hyaluronic acid, and elastin drew significant attention due to their biocompatibility, biodegradability, and non-toxic nature [52, 53]. Moreover, smart wound dressings are also designed by making composite systems with these natural polymers and various reinforcing agents [54, 57]. Yet, more research is required to translate them to clinics. In addition to these

alternatives, it was shown that sericin could be an alternatenatural polymer candidate for such applications due to its unique properties if some of the drawbacks, such as mechanical properteis, were overcome [57].

2.5 Objectives

The aim of this project was to utilize silk sericin, which was discarded as a waste material in textile industry, in biomedical applications. High temperature and pressure method was used to extract sericin. Brittleness, which is the biggest drawback of sericin, was remedied by introducing glycerol as a plasticizer at a suitable composition. Sr^{2+} and Zn^{2+} incorporated BG (which was not investigated previously in literature with sericin) and GO were used as reinforcing agents to improve the mechanical and biological properties, and antibacterial performance of the final composite films.

CHAPTER 3

EXPERIMENTAL METHODS

3.1 Materials

Bombyx Mori silkworm cocoons were purchased from Kozabirlik (Bursa, Turkey). Graphene Oxide was kindly provided from the Nanomaterials Group of Assoc. Prof. Dr. Göknur Büke in TOBB University of Economics and Technology. Glycerol solution (84-88%), zinc nitrate hexahydrate (98%), strontium nitrate (>99%), tetraethyl orthosilicate (TEOS, 99%), triethyl phosphate (TEP, 99.8%), calcium nitrate tetrahydrate ($Ca(NO_3)_2.4H_2O$, CaN, 99%), and hexamethyldisilizane were purchased from Sigma Aldrich. Dulbecco's Modified Eagle Medium (DMEM), penicillin-streptomycin, fetal bovine serum (FBS) and trypsin-EDTA were purchased from Biological Industries (BI). 3- (4,5-dimethyl-2-thiazolyl)-2,5-diphenyl-2H-tetrazolium bromide (MTT) was purchased from Abcam. Tryptic Soy Broth (TSB) and agar were purchased from Merck.

3.2 Extraction of Sericin

In order to extract sericin, high pressure and temperature method was used in the experiments. Briefly, finely cut 5 grams of *Bombxy mori* silkworm cocoons were steeped with 50 ml of DI water in a 100 ml glass bottle. Afterwards, cocoon pieces were autoclaved at 120 °C for 20 min. At the end of the autoclave process sericin solution was obtained. The obtained sericin solution was centrifuged at 7800 rpm for 10 minutes to remove the remaining fibroin and other contaminations. Finally,

30 ml of supernatant was obtained and used as the sericin solution in the experiments without any purification or concentration steps.

3.3 Preparation of Reinforcements

GO was prepared by improved Hummers' method [58]. In short, sulphuric and phosphoric acids were added to a beaker which contains graphite flakes. Then, $KMnO_4$ was added carefully in that mixture while controlling temperature under constant mixing. This reaction was continued for 2 days at 50 °C. Afterwards, the mixture was cooled, and H_2O_2 solution was added until the color of the mixture changed. Then the solution was centrifuged, and supernatant was discarded. Remaining material was washed first with HCl, and then with water and finally with ethanol. After drying GO was ready to be used.

To prepare Sr and Zn doped BG particles, alkaline solution is prepared by using a 0.66 volume ratio of distilled water to ethanol as the first solution which had a 1.4M ammonia concentration. In order to make the second solution, ethanol, TEOS, and TEP were used (TEOS/Ethanol volume ratio ~ 0.09). The second solution was then added into the first solution. After one hour of stirring, CaN was added into it, and mixed for another hour. Lastly, SrN and ZnN were added to the system as the last two ingredients to complete the process. In order to prevent unreacted compounds from remaining in the system, the precipitates were centrifuged three times with water and ethanol. Furthermore, after the drying step, the powder was calcined for 2h at 700°C.

3.4 SS/GO and SS/BG Composite Film Fabrication

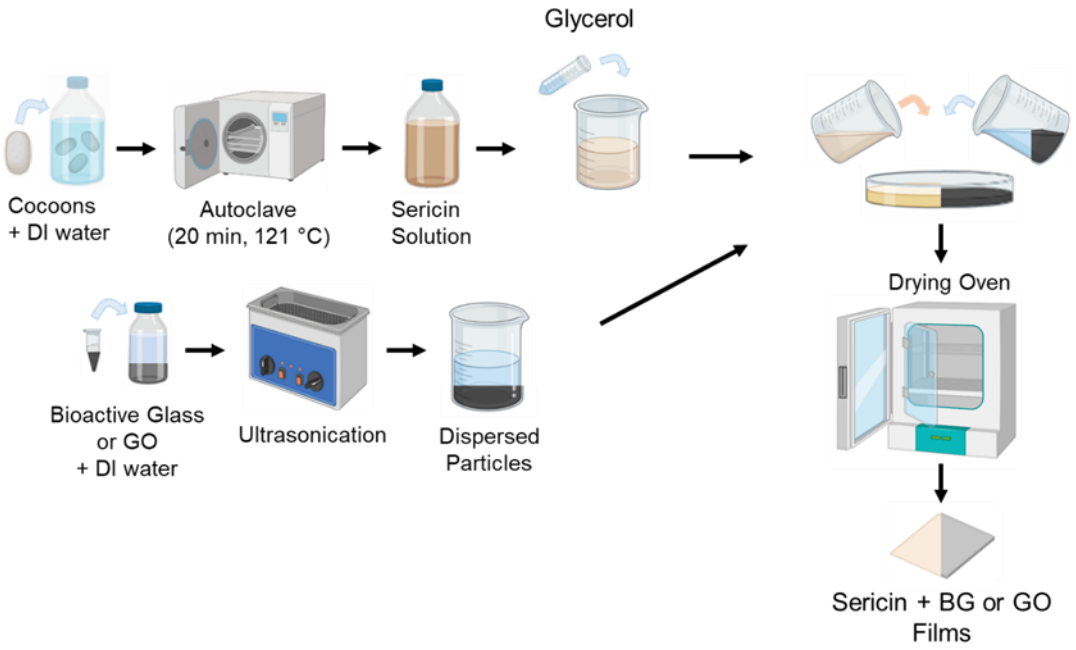

Figure 3.1 Synthesis steps used for sericin based composite films.

After extraction of sericin, 15 ml of the obtained solution was transferred to a beaker and stirred at 200 rpm. During stirring, 50% (w/w) of glycerol (with respect to sericin) is added to this solution as a plasticizing agent. At the same time, BG or GO particles were weighted. For BG samples, 3, 5 and 7% (w/w, with respect to sericin) concentrations were prepared, whereas for GO samples concentrations were selected as 0.25, 0.5 and 1% (w/w, with respect to sericin), as listed in Table 3.1. BG and GO were dispersed in DI water for 60 minutes using an ultrasonic bath. Then, these particles were combined with the sericin solution. Throughout the experiments, sericin solution was kept above 60 °C to prevent gelation. Finally, this mixture was sonicated 3 minutes in a ultrasonication bath, transferred to a petri dish, and then waited in an oven at 50 °C overnight. As a result, Sericin/BG or Sericin/GO composite films were obtained. Experimental procedure was shown in Figure 3.1.

3.5 Characterization of SS/GO and SS/BG Composite Films

3.5.1 Scanning Electron Microscopy (SEM)

Surface morphology and cross-section areas of the sericin films were investigated using an FEI Nova Nano SEM 430 model microscope. 10 kV accelerating voltage was utilized for imaging. All samples were coated with a thin layer of gold using Quorum SC7640 sputter coater for 3 minutes before SEM characterization to create an electrically conductive path.

3.5.2 Energy Dispersive Spectroscopy (EDS)

Elemental composition of the bioactive glass and sericin based composite films were identified using an energy dispersive X-ray spectroscopy (EDS) attachment to the SEM device. Thus, information about elemental content were obtained for each sample.

3.5.3 X-ray Diffraction (XRD)

Rigaku D/Max-2200 X-ray Diffractometer was used for analyzing XRD patterns of the sericin based films (before and after degradation) and reinforcements. Monochromatic Cu Kα radiation ($\lambda = 1.54$ Å) at 40 kV was used and diffraction angles (2θ) from 10 ° to 60° were scanned with 2°/min scanning rate.

3.5.4 Fourier Transform Infrared Spectroscopy (FTIR)

PerkinElmer 400 Fourier transform infrared spectrometer was used to determine molecular bonding characteristics of pure sericin, sericin/glycerol, sericin/glycerol/BG and sericin/glycerol/GO films (before and after degradation) within 4000 - 400 cm^{-1} scanning range with 4 cm^{-1} resolution using attenuated total

reflection (ATR) configuration. From changes in the fingerprint region of the spectrum, effect of secondary agents on the sericin was investigated. Also, alterations in the amide I region (1600-1700 cm^{-1}) was used to determine secondary structure, and thus, the crystallinity of the composite films were assessed. Average of four spectra for each sample was reported.

3.5.5 Mechanical Properties

Instron 5565A testing machine was used for uniaxial tensile tests for sericin based composite films according to ASTM D882 standards. Films were cut as 1 x 5 cm^2 sheets, and gauge length was adjusted to 2 cm. 25mm/s loading rate was applied using a 5 kN load cell. Six experiments were conducted for each sample. All film samples were tested in wet condition at 37 °C.

3.5.6 Thermal Analysis

Thermogravimetric analysis (TGA) was conducted for thermal analysis of sericin based composite films. TA Instruments SDT 650 Simultane TGA device was used with a heating rate of 10°C/min between 25-600 °C in N_2 environment. Information about thermal stability, dehydration, adsorption and decomposition can be obtained from the mass change curves as a function of temperature.

3.5.7 Swelling and Degradation of Composite Films

Sericin based composite films were cut as 2.5 x 2.5 cm^2 sheets. Initial weights of the samples were measured and they were placed in 1xPBS (pH = 7.4). After 1, 24 and 72 hours, wet and dry weights were measured to determine swelling and mass loss behavior, respectively, using the following equations:

$$\%swelling = \frac{Wf-Wi}{Wi}\ x\ 100 \qquad \%mass\ loss = \frac{Wi-Wf}{Wi}\ x\ 100$$

(Wi = initial weight and Wf = final weight)

3.5.8 Cell Culture and Metabolic Activity

To evaluate the toxicity of the sericin films, fibroblasts (L929, ATCC number: CCL-1, passage number 21) were cultured using growth medium (DMEM, Sigma Aldrich D6429) supplemented with 10% fetal bovine serum (FBS, Biological Industries, 04-001-1A) and 1 % penicillin-streptomycin (Biological Industries, 03-031-1B) under 5 % CO_2 at 37 °C. All samples were sterilized with UV light twice for 30 minutes from the top and bottom sides.Then, samples were transferred to DMEM and kept for 72 hours at 37 °C for extraction. Fibroblasts were seeded to 96 well plates at a density of 10.000 cells/cm^2 and cultured for 24 hours in a humidified environment. Afterwards, media containing the sericin film extracts were added onto the cells and incubated up to 7 days *in vitro*. For determination of cytotoxicity, 3-(4,5-dimethyl-2-thiazolyl)-2,5-diphenyl-2H-tetrazolium bromide (MTT) assay was used. After 1, 3, 5 and 7 days of culture, culture media were aspirated, and each well was rinsed with 1xPBS and 125 µL MTT solution was added. After 4 hours of incubation with the MTT solution, formazan crystals formed. 125 µL of 2-propanol-HCl solution was added to each well to dissolve formazan crystals. Using Thermo Scientific Multiskan GO spectrophotometer, optical density values of each well were measured at 570 nm. Experiments were conducted three times using three samples each time.

3.5.9 Antibacterial Properties

Sterile sericin films were transferred to 0.3% (w/v) Tryptic soy broth (TSB). After 72 hours, extracted medium was added to 96 well plates. *Staphylococcus aureus* (*S. aureus*, ATCC 25923) and *Escherichia coli* (*E. coli*, ATCC 10536) were used as gram-positive and gram-negative bacteria, respectively, to assess antibacterial properties of the films. Each bacteria were streaked onto LB-agar to form colonies,

and then single colony was isolated and inoculated into 3% (w/v) TSB and cultured 18 hours with 200 rpm at 37 °C. Bacteria solution density was adjusted with 1xPBS to optical density (OD) = 0.11 and seeded on extracted media placed in 96 well plates and incubated for 24 hours at 37 °C. Afterwards, the cultured bacteria solutions were diluted using 1xPBS up to 5 logs and seeded onto sterile LB-agar plates. Seeded bacteria were incubated at 37 °C for 24 hours. Finally, colonies were counted and compared with control groups without extract samples.

3.5.10 Statistical Analysis

Experiments were conducted at least three times and results were reported as mean ± standard deviation. Statistical analyses were performed with ANOVA using Tukey's post-hoc test with significance based on $*p \leq 0.05$ in SPSS software.

Table 3.1 Composition of sericin based composite films.

Sample	Content
SS	Sole Sericin
SSG	Sericin + 50%(w/w) Glycerol
SSG-0.25GO	Sericin + 50%(w/w) Glycerol + 0.25%(w/w) GO
SSG-0.5GO	Sericin + 50%(w/w) Glycerol + 0.5%(w/w) GO
SSG-1GO	Sericin + 50%(w/w) Glycerol + 1%(w/w) GO
SSG-3BG	Sericin + 50%(w/w) Glycerol + 3%(w/w) BG
SSG-5BG	Sericin + 50%(w/w) Glycerol + 5%(w/w) BG
SSG-7BG	Sericin + 50%(w/w) Glycerol + 7%(w/w) BG

CHAPTER 4

RESULTS AND DISCUSSION

The main purpose of this study was to utilize sericin, which is considered as a waste in textile industry for a long time, for biomedical applications due to its unique properties. Sericin was extracted from *Bombxy mori* silkworm cocoons with high temperature and pressure method thanks to its water solubility by autoclaving. During fabrication of sericin based films, glycerol was used as a plasticizing agent to overcome the high brittleness of sole sericin. Moreover, graphene oxide and Sr and Zn incorporated bioactive glass were used as second phase reinforcing agents to improve mechanical and antibacterial properties of the film samples. As a result, flexible sericin based composite films were fabricated as shown in Figure 4.1. The effect of each one of these modifications on final sericin films was examined in the following headings.

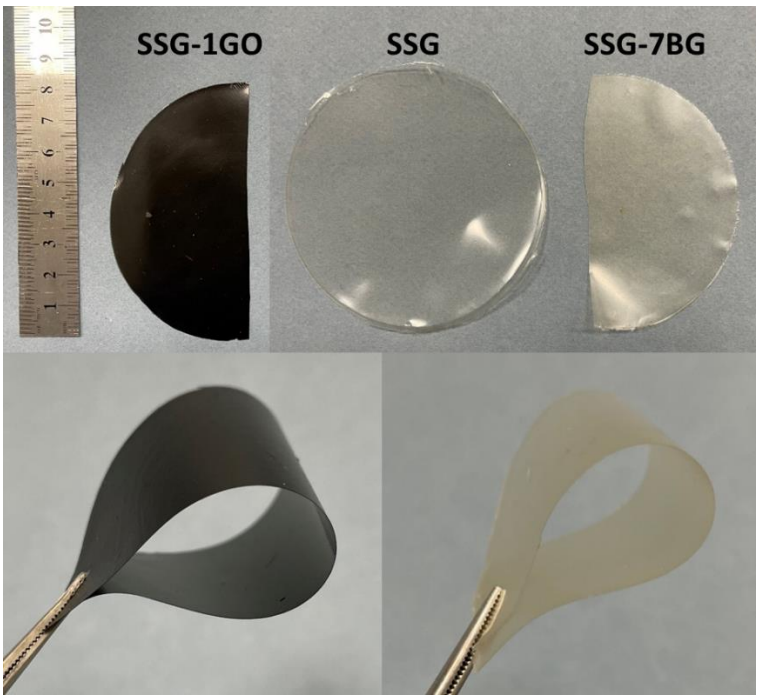

Figure 4.1 Flexible sericin based composite films.

4.1 Effect of Glycerol

SEM images of sole (SS) and 50% glycerol added (SSG) sericin films from its cross-section were shown in Figure 4.2. Average thickness of the films were measured as 58 ± 5 µm by using ImageJ software. It is clearly seen that, sole sericin has a brittle fracture surface whereas SSG films show ductile behavior during cutting after the 50% glycerol addition. Although there seems to be a slight increase in the surface roughness of the films after addition of glycerol, in both conditions surfaces of the films can be considered as smooth since no pattern formation is occured. Moreover, no phase seperation was observed, which indicates the good compatibility between glycerol and sericin

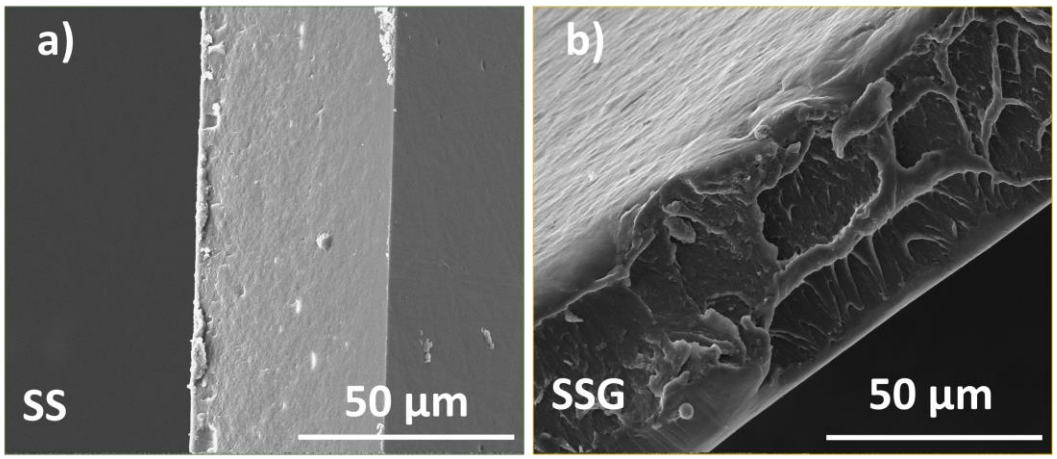

Figure 4.2 Cross-sectional SEM images of a) SS and b) SSG films.

In order to see the possible effects of glycerol on sericin films and decide the required amount that was used in this study, 3 different film groups were fabricated by using 30, 50 and 70% (w/w) of glycerol with respect to sericin before the experiments.

From the XRD spectra in Figure 4.3, it is evident that increasing glycerol concentration in the films increases the sharpness of the characteristic peak of sericin at 2Θ=19° [28]. This trend indicates that addition of glycerol can cause an increase in the regularity in the structure of the resulted films which can be correlated with crystallinity of sericin. Yet, to support these results, secondary structures of these films should be investigated since crystallinity of sericin is also related with its β-sheet content. [27], [28].

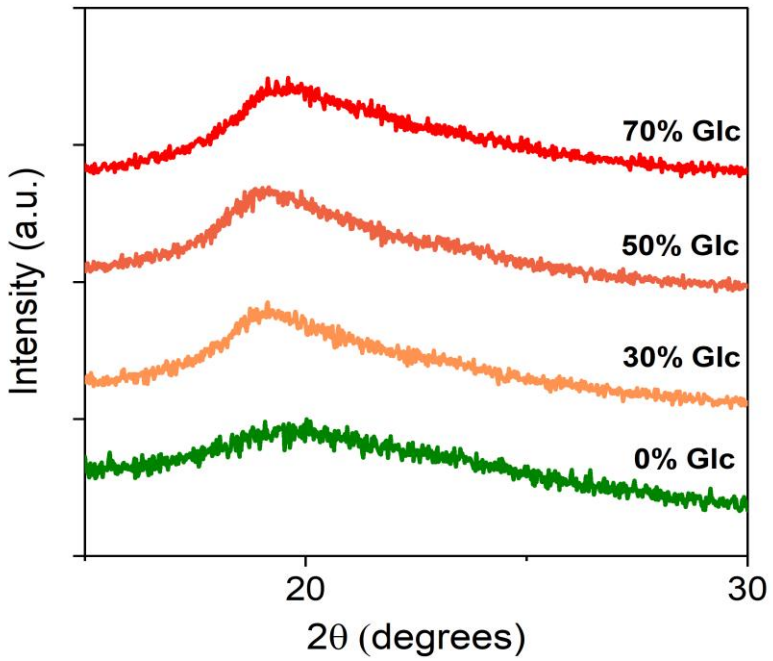

Figure 4.3 XRD spectra of sericin based samples with increasing glycerol concentration.

It is reported that, secondary structures of sericin can be decided by the shifts of amide I region in FTIR peaks (1600-1700 cm^{-1}) [27], [28]. While the peak at 1619 cm^{-1} is related with β-sheet structure, peak at 1645 cm^{-1} is found out to be related with random coil structure [28, 39]. Therefore, after normalization, the ratio of the peak at 1619 to 1645 gives the idea about overall crystallinity of sericin. From the FTIR results of the sericin/glcerol films (Figure 4.4), it can be seen that with the

increasing glycerol concentration, amide I peak shifts to 1619 cm^{-1} which indicates that addition of glycerol induces the β-sheet formation. In their works, Zhang *et al.* [27] and Yun *et al.* [28] found the same trend with increasing glycerol concentration. This results also supports the XRD data. It was known that glycerol cause protein compaction [59] which is expected to reduce the flexibility. However, due to its hygroscopic nature, glycerol prevents the evoporation of water molecules during film casting which increases the moisture content of resulted products. Since water is also a strong plasticizer for many natural polymers, it can enter between sericin molecules (especially from random coil regions) and induce plasticity by increasing the free volume [28]. That effect was in accordance with the study of Teramoto *et al.* which claims that β-sheet structure was stabilized by water due to the intermolecular hydrogen bonding of hydrophobic regions of sericin, namely Ser and Thr sites [60]. Thus, flexibility of the films could be increased as a result of the synergistic effect of water and glycerol.

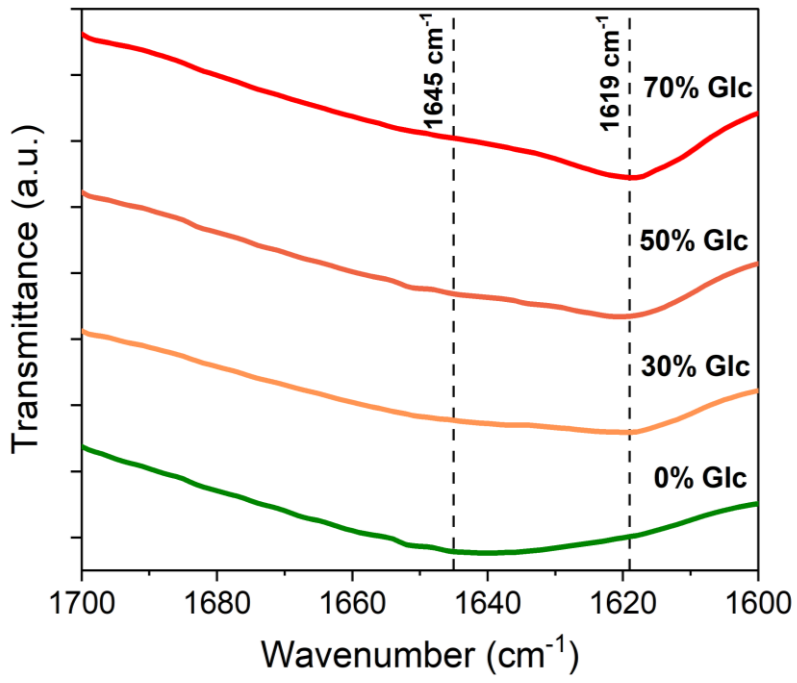

Figure 4.4 FTIR spectra of the amide I region of sericin based films with increasing glycerol concentration.

Although crystallinity was increased with the addition of glycerol, due to its plasticizing effect it deteriorates the mechanical and thermal properties of the resulted films. From the TGA curves In Figure 3.6 it is seen that thermal decomposition of pure sericin is started mainly at 230 °C. Yet, after 50% glycerol addition that temperature decreases up to 195 °C (Figure 4.5a). This could be the result of the glycerol loss, which can easily be seen as an extra event in the first derivative of TGA curves (Figure 4.5b) as well as the increased chain mobility of sericin. Glycerol breaks the existing hydrogen bonds and forms new ones between sericin and glycerol which increases the free volume and consequently the mobility of chains. Also, stable β-sheet structure was diminished due to vaporizing of water molecules until 100 °C. Combination of these effects cause earlier thermal decomposition of SSG films. That mobility increase also has a negative effect on the mechanical properties of these films.

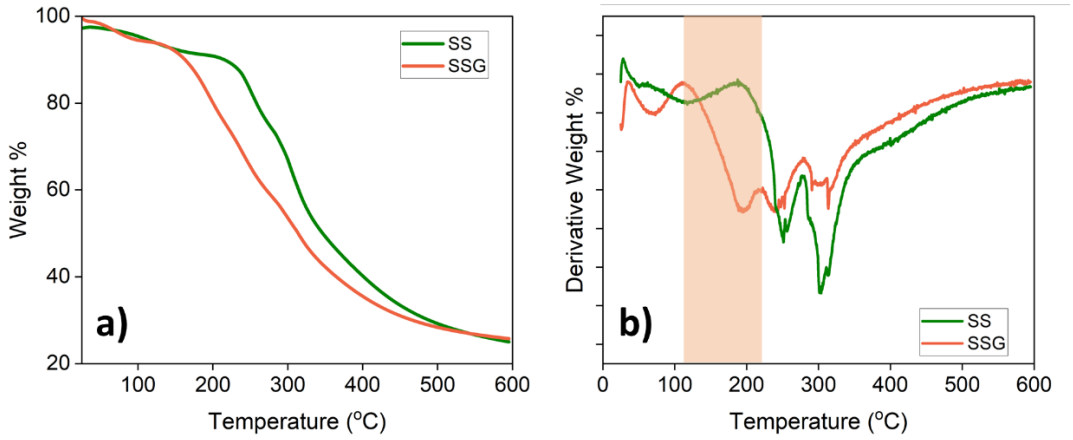

Figure 4.5 a) TGA curves and b) derivatives of the TGA curves for SS and SSG films.

Samples were soaked into 1xPBS for 72 hours in order to observe the degradation performance of the films. It was evident from the cross-sectional SEM images of both SSD and SSGD films in Figure 4.6 that after soaking, plasticized films were

also showed brittle like behaviour. Moreover, after degradation in PBS for 72 hours, an irregular shaped pattern was observed on the top surface of the SSGD films. This change can be caused by the seperation of glycerol from the system since this irregular shaped pattern was observed throughout the surface homogenously.

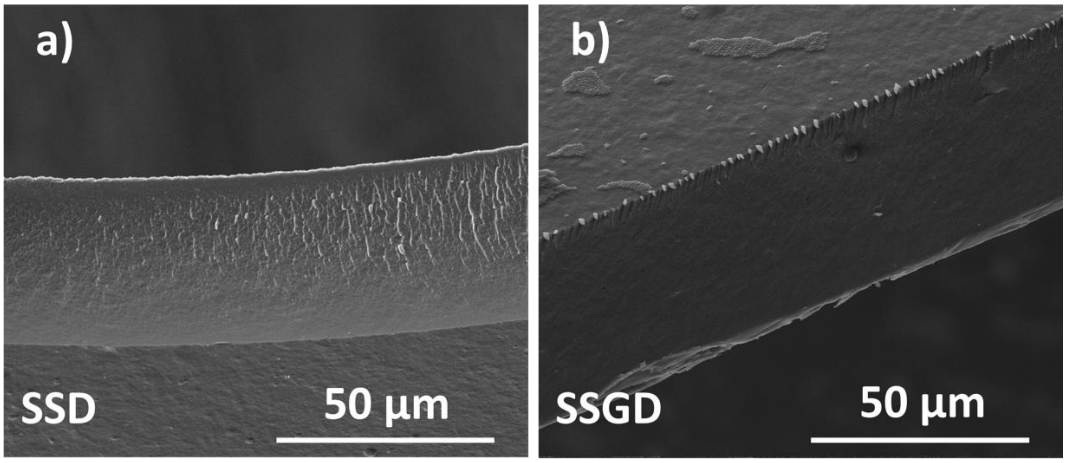

Figure 4.6 Cross-sectional SEM images of a) SSD and b) SSGD films (soaked in 1xPBS for 72 h).

Comparing the FTIR patterns of SS, SSG and SSGD samples (Figure 4.7), it can be seen that two peaks were appeared at 1108 and 995 cm^{-1} which are related to acyl and phenyl C-O and C=C bonds respecitively [61]. They demonstrated the successful combination of sericin and glycerol. However, after degradation of the films in 1xPBS in 72 hours, these peaks were disappeared and FTIR pattern of the degraded samples becomes like the initial SS sample. Which indicates that glycerol left the system during the degradation. Yet, in the experiments, it was seen that films could maintain their flexibility in wet form after these processes. This can imply that glycerol cannot leave the system completely or water molecules continued to act as a plasticizer after the diffusion of glycerol.

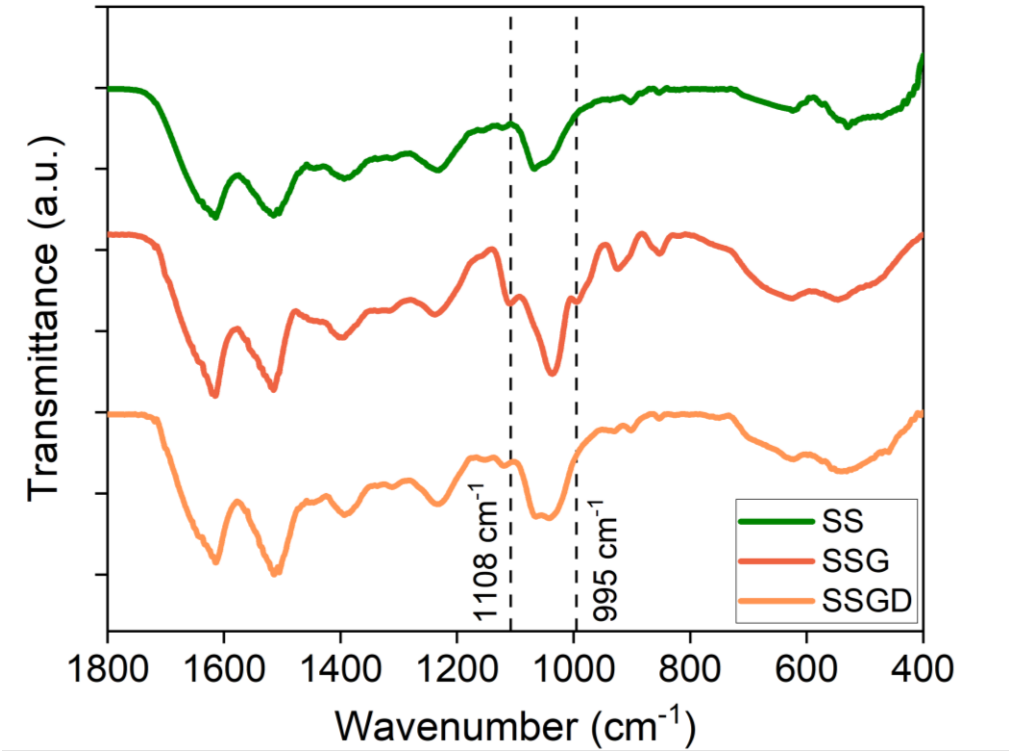

Figure 4.7 FTIR spectra of SS, SSG and SSGD films.

Mechanical properties, that are directly related to chain mobility, were also an important criterion for the fabricated films besides their flexibility. Thus, 50% glycerol, which was found as the minimum amount that provides the required flexibility, was choosen as the fixed glycerol concentration for all of the produced sericin based composite films.

4.2 Effect of GO on SS Films

4.2.1 Graphene Oxide (GO)

Surface topography of GO was examined by scanning electron microscopy. GO sheet with wrinkles clearly seen in the SEM images in Figure 4.8a. Aggregated thin sheets forms a disordered solid. Moreover, XRD pattern for graphene oxide shows a strong peak at 2Θ=12.1° which corresponds to 0.8 nm interlayer spacings. That indicated the existence of oxygen containing functional groups in the GO (Figure 4.8b). However, the peak at 2Θ=26° (0,33 nm interlayer spacing) indicates that some portion of non-oxidized graphite flakes were also present in the GO phase [62].

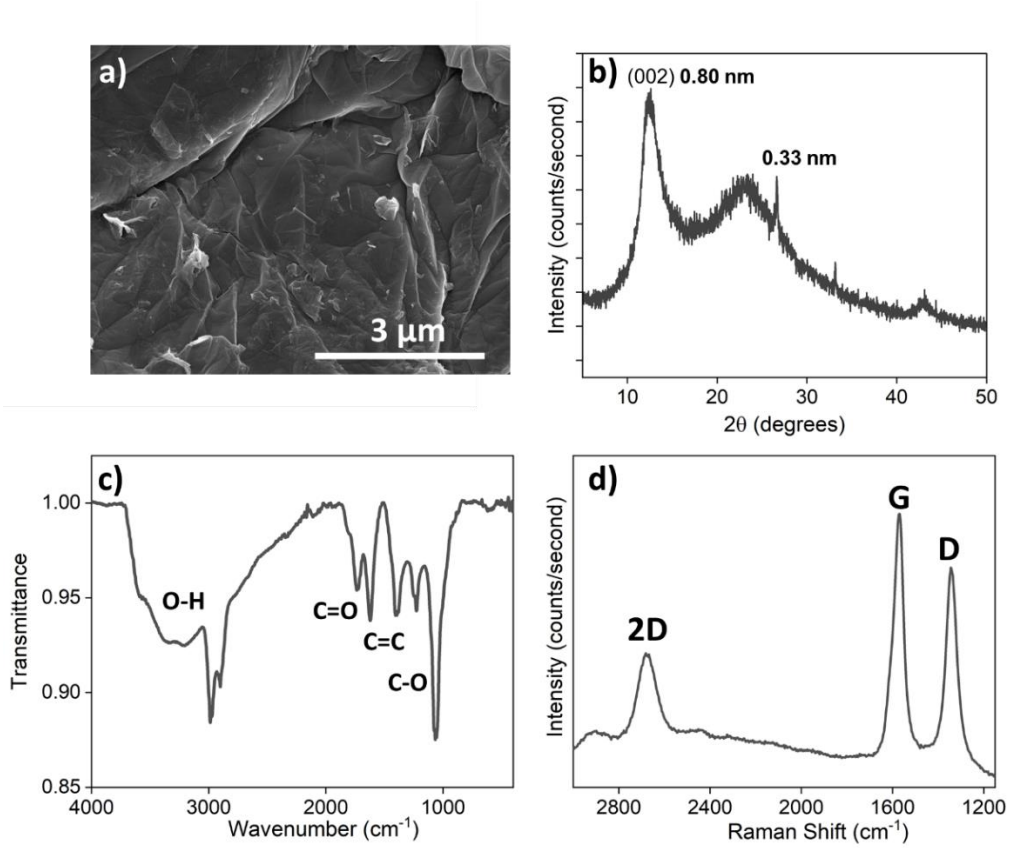

Figure 4.8 a) SEM image, b) XRD, c) FTIR and d) Raman spectra of GO.

In FTIR curve of GO (Figure 4.8c), peaks were observed at 1814, 1731 (C=O stretching), 1621 (non-oxidized C-C bonds and adsorbed water), 1405 (C-OH), 1250 (C-O-C), 1226 and 1067 (C-O) cm^{-1}. The peaks further proofed the presence of oxygen containing functional groups such as carboxyl, hydroxyl, carbonyl or epoxy [35]. Broad band at 3400 cm^{-1} corresponds to O-H stretching due to the adsorbed water on the surface. Moreover, three main peaks were observed in Raman spectra of GO particles (Figure 4.8d) show characteristic G peak at 1575 cm^{-1} corresponding to sp^2 graphitized structure and D peak around 1350 cm^{-1} due to defects and disorders due to lattice distortion. The broad 2D band 2680 cm^{-1} also implies the disruption of stacking order of graphite after oxidation [35, 37, 62, 63].

4.2.2 SSG-GO Composite Films

Cross-sectional areas of SS-GO samples were examined by scanning electron microscopy. It is seen in Figure 4.9, SSG-GO films have average thickness of 54 ± 6 μm. They also show ductile surface characteristics due to 50% glycerol addition. Although there were some areas of aggregation, it can be said that GO phase was distributed uniformly throughout the sericin films.

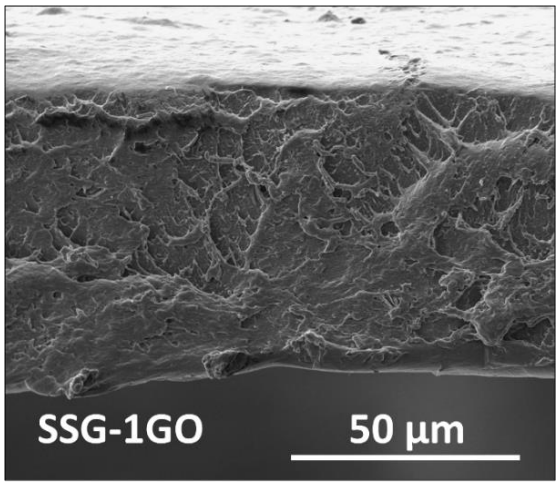

Figure 4.9 Cross-sectional SEM image of SSG-1GO sample.

Uniaxial tensile test results show that addition of GO increases the elastic modulus of resulted films from 16.7±0.9 MPa up to 19.3±1.9 MPa while decreasing their ductility up to one thirds (Figure 4.10). This might be the result of the hydrogen bonding between amino and hydroxyl groups of sericin and epoxy, hydroxyl and carboxyl groups in GO. Due to these interfacial forces a portion of applied load can be transferred to secondary reinforcement phase [64]. Yet, to succesfully make this load transfer, GO should be extremely well dispersed in the films. Thus, the increase in modulus can only be occured as a result of decreasing chain mobility of the sericin after addition of reinforcing GO phase. That decrease in chain movement also reduces the plasticizers effect. Nevertheless, since enough flexibility is maintained in the films during experiments this phenomenon cannot constitue any problem. In addition, strong interactions between GO and sericin can restrains intermolecular bonding of sericin thus reduces β-sheet structures and crystallinity [29]. The preservation of flexibility may cause because of that condition.

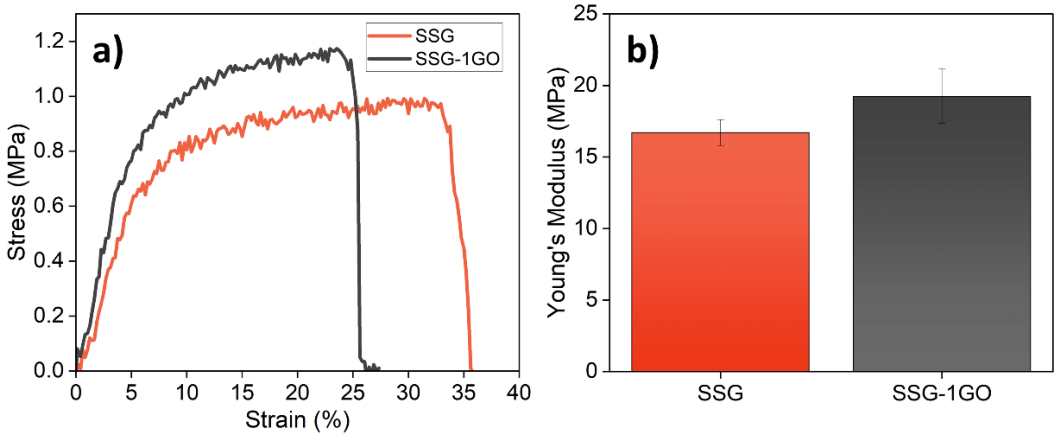

Figure 4.10 a) Stress-strain curves and b) Young's modulus values of SSG and SSG-1GO samples.

TGA curves of SSG-GO samples show 4 distinct regions. Up to 100 °C, weight loss occurred due to vaporization of adsorbed water. Around 195 °C glycerol

vaporizes which can be seen as an extra peak in first derivative of TGA curves (Figure 4.11). Thermal decomposition of sericin starts at 230 °C. Amorphous regions decomposes more quickly than crystalline regions (clearly seen in the derivative TGA curves) which can decompose around 320 °C. Since GO is a thermally unstable material [65] due to the pyrolisis of oxygen containing fuctional groups with the formation of CO, CO_2 and steam [66], SSG-GO films decompose earlier than SSG and SS films. From the TGA curves, it can be seen that while addition of glycerol decreases the main thermal decompsition temperature of the films from 230 °C to 160 °C, 1% GO addition slightly decreases that temperature to 155 °C (Figure 4.11). Moreover, since GO starts to decompose earlier than sericin [66], after the experiment no weight loss difference was observed between SSG, SSG-GO films.

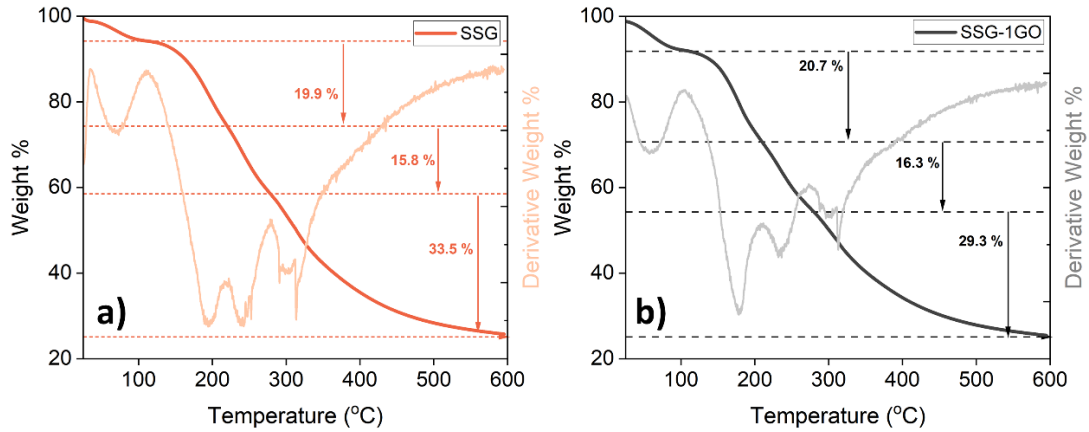

Figure 4.11 TGA curves and derivatives of TGA curves for a) SSG and b) SSG-1GO samples.

After degradation in 1xPBS, brittle like surface behaviors were observed from the cross-sectional SEM image in Figure 4.12. Some thin voids were also seen after degradation, they may arise due to the detachment of aggregated GO during the degradation where glycerol diffuses out and swelling occurred at the same time. Moreover, a non-ordered but homogenously distributed pattern was seen at the top

surfaces of the films in dry state. This effect can be caused by the seperation of glycerol since similar pattern was observed from the degradation of SSG films whose FTIR pattern indicates firstly glycerol leave sthe system during degradation.

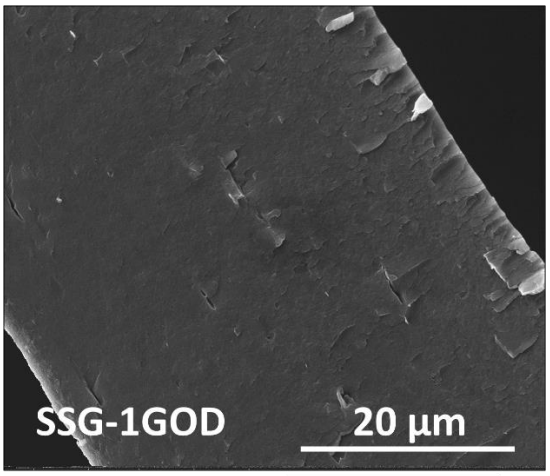

Figure 4.12 Cross-sectional SEM image of SSG-1GOD sample.

Water retention is one of the desired properties of sericin especially for wound dressing applications. Since glycerol increases the crystallinity of the films and GO can decrease the chain mobility their effect on swelling behavior could be crucial. Nevertheless, comparing the % swelling raitos (Figure 4.13a), SSG and SSG-0.25GO samples show no significant difference. While SS-1GO samples were the lowest water retention ability after 3 days, SS-0.25GO ones showed the highest % swelling up to 130%. Overall, all samples has a average swelling ratio of 100-120 %. Which means they can contain water more than their initial weigths in the wet form. % swelling showed a decreasing trend with increasing GO content. This results implies that strong hydrogen bonding with GO makes the penetration of water molecules difficult. Also, 1% GO did not disrupt the β-sheet formation dramatically.

Degradation was another important parameter for sericin since it is a biodegradable material. Effect of %GO in the mass loss of SS films was shown in Figure 4.13b. From that results, it is seen that all films regardless of their GO content lost nearly 35-40% their initial weights in the first hour of degradation. Since there is a 50% glycerol were present in the films at the first place and XRD and FTIR results showed that it leaves the system during the degradation, this results showed that glycerol was seperated as early as 1 hour in that degradation period. After that, up to 3 days samples showed no significant weight change. Similar cocncentration dependent trend was also seen for mass loss.

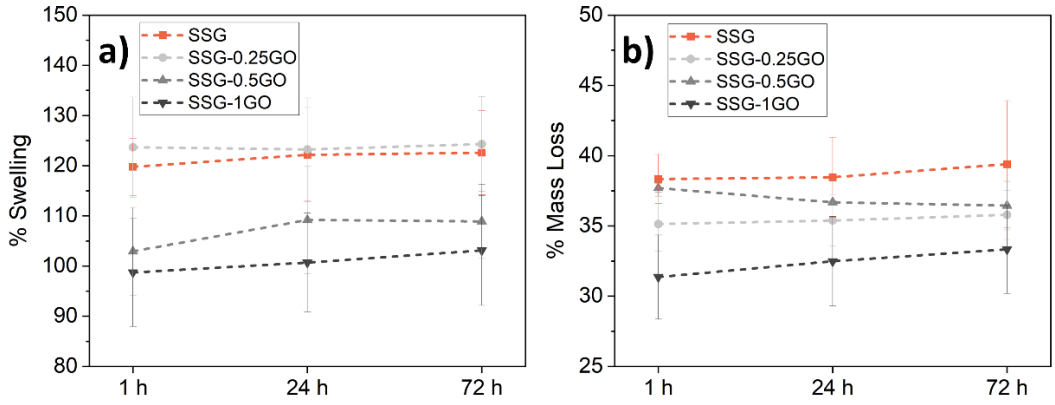

Figure 4.13 a) % swelling and b) % mass loss of SSG and SSG-GO samples up to 72 h in 1xPBS.

There were no significant diffenrence in X-ray diffraction patterns between SSG-GO films (Figure 4.14). They all showed a major peak at 2Θ=21° and a small bump at 2Θ=14°. Since it was known that glycerol increases β-sheet content and crytallinity of sericin based films, that major peak can be caused by increasing regularity. Moreover, by comparing the XRD patterns of SS, SSG, SSG-1GO and SS-1GOD films in Figure 3.14, it is evident that after degradation the peak at 2Θ=21° diminishes while 2Θ=14° one becomes dominant which is also the major peak of SS. Thus, it can be said that due to the loss of glycerol, ordered structure of

the sericin based films were declined after degradation. However, GO was not showed any change in the XRD spectra. Although, an interaction between functional groups of GO and sericin were expected, 1% GO addition cannot be sufficient to detect in XRD.

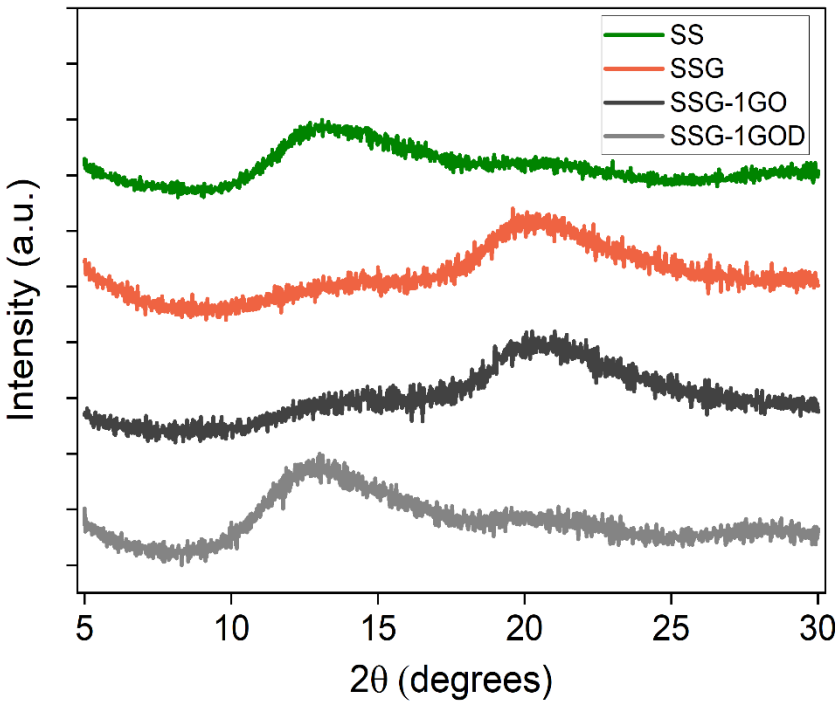

Figure 4.14 XRD spectra of SS, SSG, SSG-1GO and SSG-1GOD samples.

All SSG-GO films with changing graphene oxide concentrations showed similar FTIR patterns. Peaks at 1108 (C-O) and 995 (C=C) cm^{-1} are also present in their results since they contain 50% glycerol. Similar to SSG ones, with the degradation these peaks were fade out and the patterns became like SS (Figure 4.15) due to glycerol seperation. After degradation, a very slight peak was seen at 1815 cm^{-1} which was also present in the FTIR cureve of graphene oxide with a small shift (Figure 3.8) but it did not considered as main FTIR peaks of GO in the literature. Nevertheless, it was too hard to detect and cannot provide enough informaiton.

Apart from that, since sericin has similar side groups with the functional groups of GO, though there were some intensity changes, no additional peak was detected as a result of GO addition.

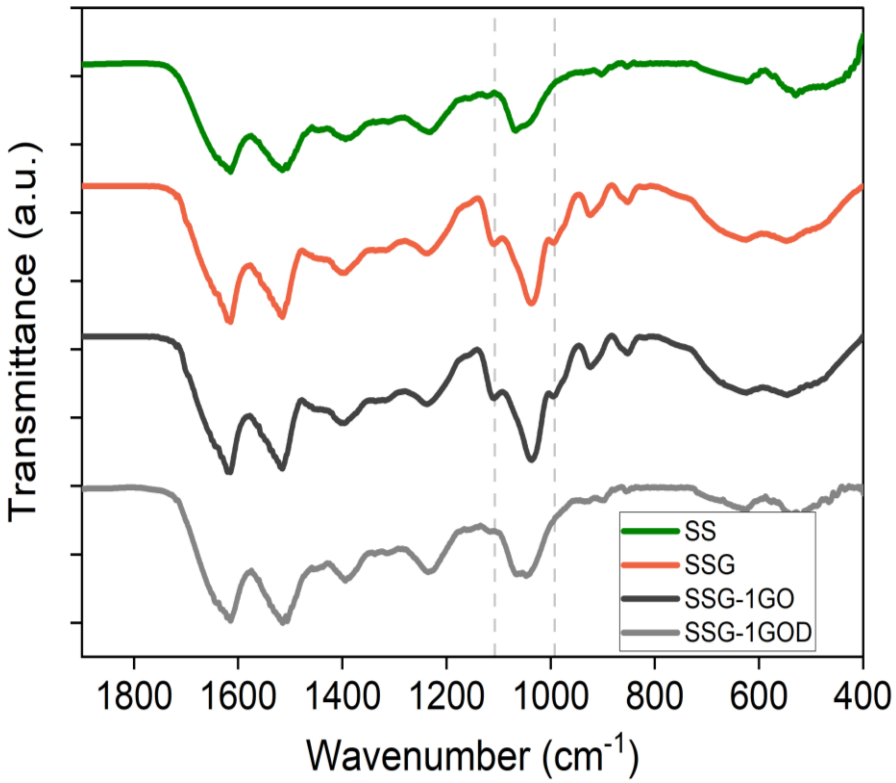

Figure 4.15 FTIR spectra of SS, SSG, SSG-1GO and SSG-1GOD samples.

In order to determine cytotoxicity of SS-GO films, MTT assay was used. 0.01g/ml extracts of all samples were prepared in DMEM and L929 fibroblast cells were cultured by using these media up to 7 days. Indirect contact results (Figure 4.16) demonstrated that SSG-GO films show no toxicity on fibroblast cells. All groups have similar adhesion and proliferation patterns with the control group which was seeded on a treated polystryrene (TCP) surface and cultured with regular DMEM medium.

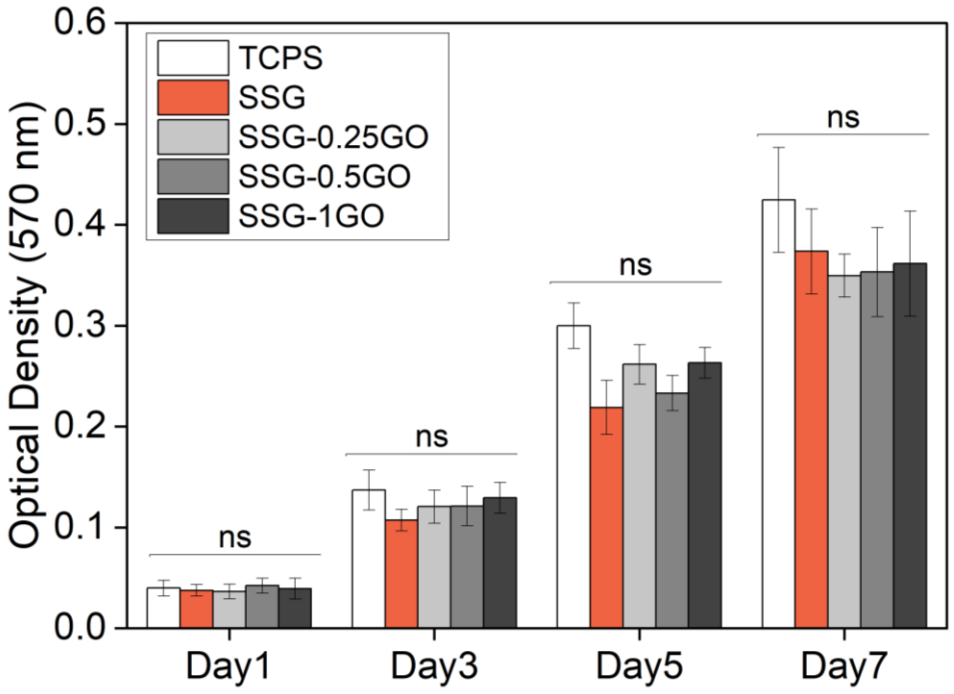

Figure 4.16 Viability of L929 fibroblasts up to 7 days *in vitro*. Values are mean ± SD (n=3), ns: non-significant.

For the evaluation of antibacteral activity of SSG-GO films, *s. aureus* was used as gram positive and *e. coli* as the gram negative bacteria in the experiments. 0.01g/ml extracts of all SSG-GO samples were prepared in 0.3% TSB media. After culturing gram positive and negative bacteria with these media, resulted colony forming unit numbers were counted on agar plates after serial dilutions and antibacterial activities of these films were investigated.

All samples show an antibacterial activity against *s. aureus.* While 0.25% GO decreases the CFU amount up to 46%, 0.5% GO show a significant decrease of 54% with respect to non GO containing control group. 1% GO also decreases the colony formation up to 27% (Figure 4.17). This antibacterial effect could be caused by the ROS formation due to the interaction of functional groups of GO and bacterial cells [33], [35]. Also, small amounts of aggregated GO were detached

during extraction (Figure 4.12) which could induce the direct contact antibacterial mechanism [63].

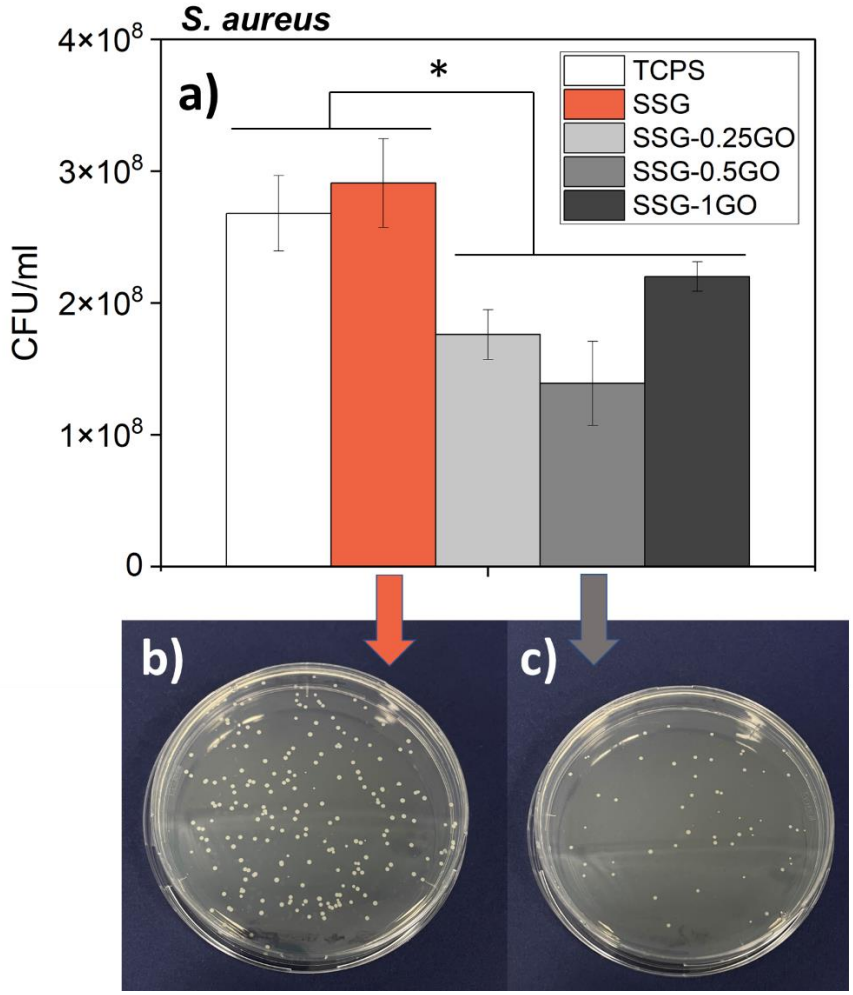

Figure 4.17 a) *S. aureus* colony counts for SS-GO films and (b-c) photographs of agar plates for b) SSG and c) SSG-0.5GO samples at 24 h of culture. Values are mean ± SD (n=3), *p< 0.05.

Similarly, All GO samples show antibacterial activity against the gram *negative e. coli*. Increasing GO concentration from 0.25% to 1% decreases the number of formed colonies from 33% to 48%. CFU counting results can be seen in Figure 4.18. Also, comparison of colonies on agar plates for SSG and SSG-1GO samples

were provided as an example of the visual difference between these groups. Increasing GO concentration, increases the antibacterial effect as expected. Same mechanisms with gram positive tests could also be a factor for these samples.

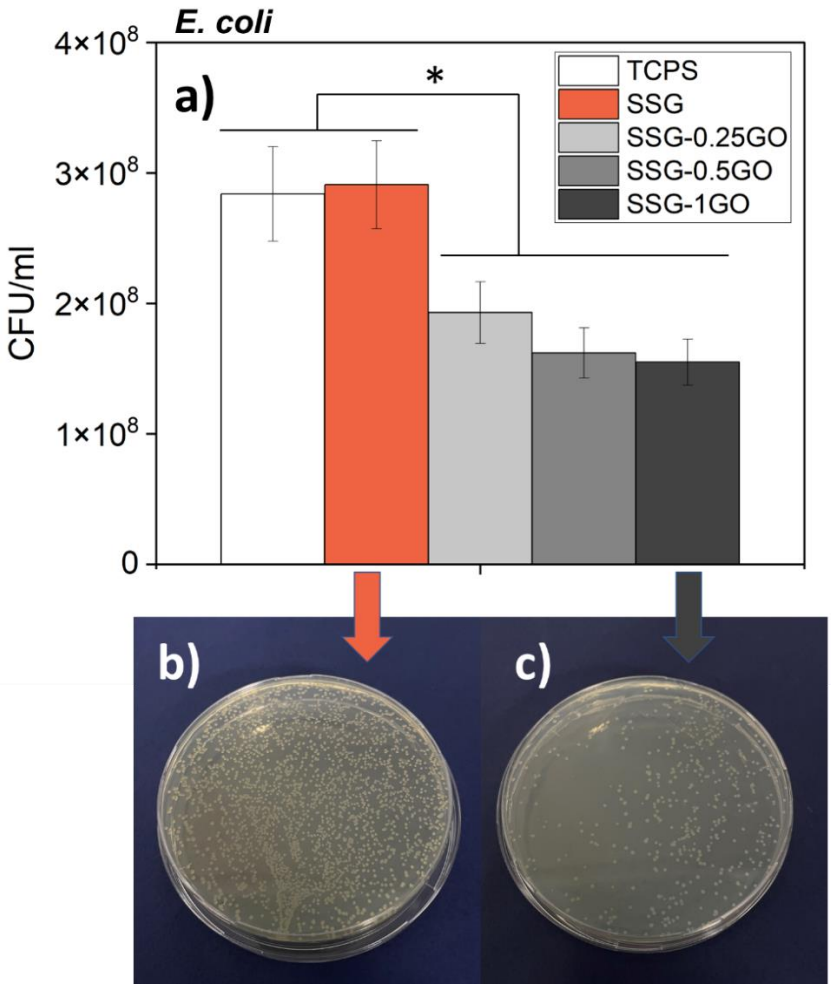

Figure 4.18 a) *E. coli* colony counts for SS-GO films and (b-c) photographs of agar plates for b) SSG and c) SSG-1GO samples at 24 h of culture. Values are mean ± SD (n=3), *$p< 0.05$.

4.3 Effect of BG on SS Films

4.3.1 Sr and Zn Doped Bioactive Glass (BG)

SEM images (Figure 4.19a) shows the spherical morphology of the BG particles that were used in the experiments. Particle sizes of BG were measured as 420 ± 10 nm. In in their EDS results (Figure 4.19b) building block elements like Si, O, Ca and P of BG can be detected as well as small amounts of the doping elements Sr and Zn in the produced BG particles.

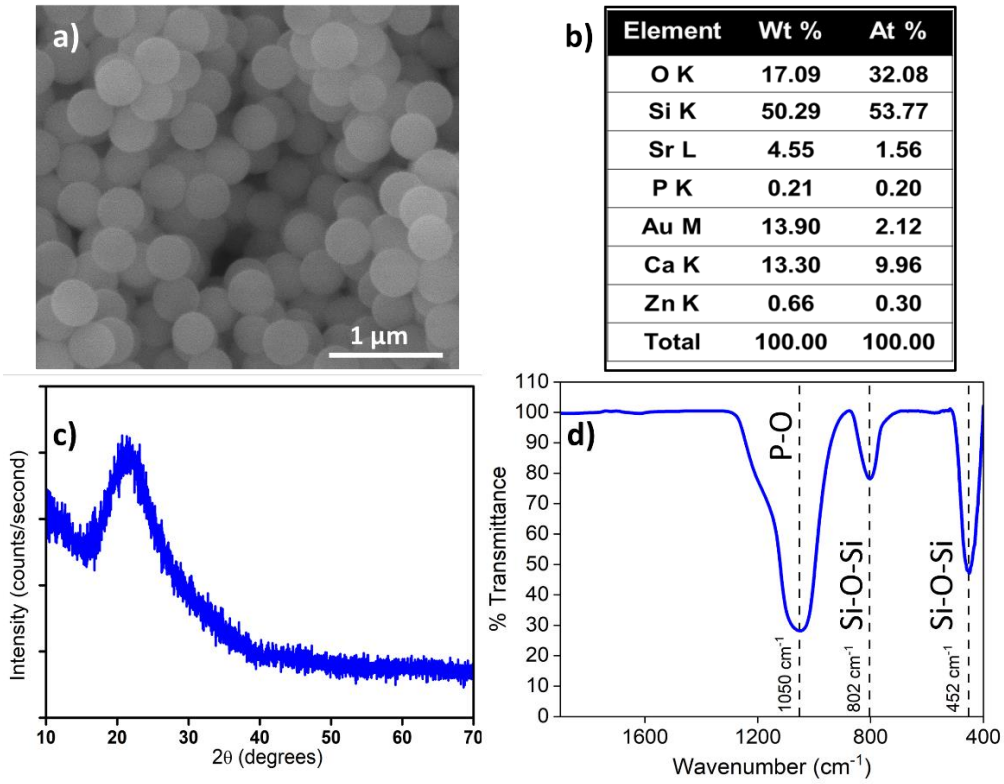

Figure 4.19 a) SEM image, b) EDS analysis, c) XRD and d) FTIR spectra of BG particles.

One large amorphous silica hump at 2Θ=21° was observed in the XRD pattern of the BG particles (Figure 4.19c) which indicates that no extra crystalline phase was formed. Also, three peaks of BG can be seen in the FTIR spectra. Since major component of the BG particles is Si, Si-O-Si bands clearly seen at 802 and 452 cm^{-1}. Besides, asymmetric P-O band were present at 1050 cm^{-1} due to the phosphate component of the BG (Figure 4.19d). That results further confirms that no additional phase was formed during the production of BG.

4.3.2 SSG-BG Composite Films

SEM images of SSG-BG films were taken from the cross-sectional areas of the samples (Figure 4.20a,b). Thickness of the films were measured as 61 ± 5 μm using ImageJ software. Cross-sectional images of the films show a ductile fracture behavior due to glycerol content. Due to their size (420 ± 10 nm) and round shape, second phase in these images were belong to bioactive glasses. Moreover, from the same cross-sectional images (Figure 4.20b) it is clearly seen that bioactive glasses show no agglomeration and distributed evenly throughout the composite film. This was an indicator of sufficient dispersion during sonication.

EDS results of the SSG-BG films in Figure 4.20c proves that spherical particles in SEM images were the bioactive glasses since they contain elements like Si and Ca, which were not belong to sericin. Due to sensitivity of sericin to high voltages, only large area EDS results could be obtained. Thus, very low signals can be collected from the doping elements like Zn.

In addition, bioactive glasses form a texture on the films, comparing to SSG samples, SSG-BG ones have rougher surfaces and round bioactive glass particles can easily be observed from their SEM images. The ones near the surface can be seen as brighter than inside ones.

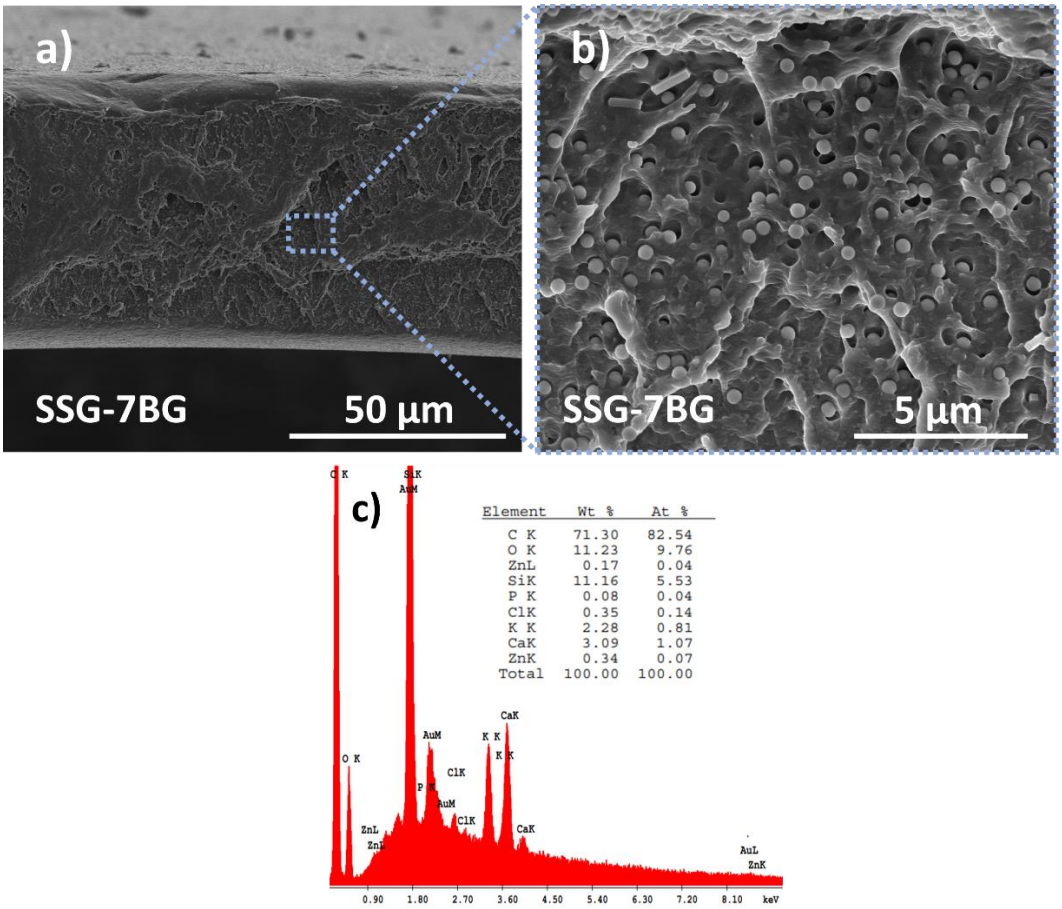

Figure 4.20 (a-b) Cross-sectional SEM images and c) EDS spectra of SSG-7BG samples.

Mechanical properties of SS-BG samples were investigated by uniaxial tensile test. The results show that BG addition increases the Young's modulus of sericin based films from 16.7±0.9 MPa up to 22.4±0.6 MPa (Figure 4.21) while decreasing the % elongation. This increase was crucial since elastic modulus was an important parameter for tissue engineering applications and the results proofed that mechanical properties of plasticized sericin can be further increased near the desired values for skin [67] via reinforcements. That incerease could be the result of reduced chain movement of sericin molecules due to the added BG particles in between them. Also, due to the excellent dispersion of BG particles, small portion of the applied load might be distributed to BG phase. The decrease in chain

mobility also negatively effect the plasticizers activity. However, since sufficient flexibility was maintained in the films it could be acceptable.

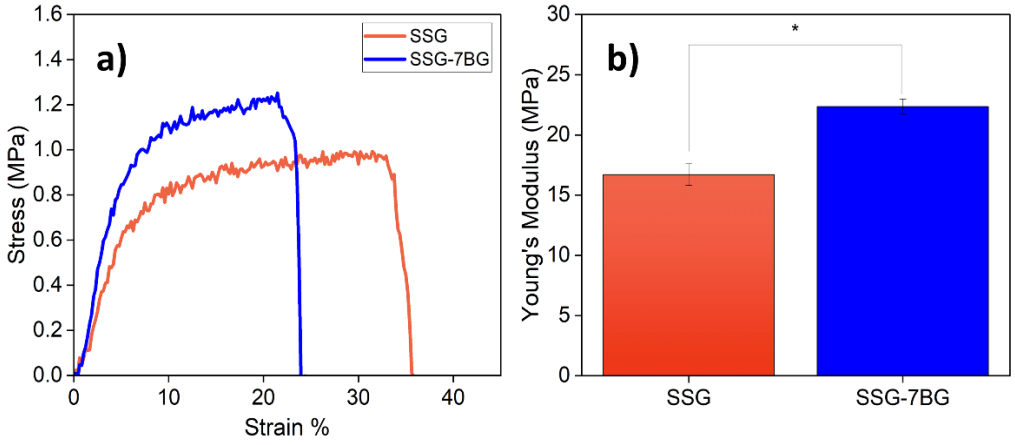

Figure 4.21 a) Stress-strain curves and b) Young's modulus values of SSG and SSG-7BG samples.

TGA of SSG-BG samples also show 4 distinct regions. Adsorbed water vaporization cause the weight loss up to 100 °C. Glycerol vaporization starts around 195 °C which can be seen as an extra peak in first derivative of TGA curves (Figure 4.22). Thermal decomposition of sericin starts at 230 °C. Fist, amorphous regions decomposes, then crystalline regions (clearly seen in the derivative TGA curves) starts to decompose around 320 °C. Similar to SSG-GO samples, addition of glycerol reduces the thermal decompsition temperature of SS from 230 °C to around 198 °C. However, even 7% BG addition did not change decomposition temperature further. Approximately 6 w% difference between SSG and SSG-BG was observed at the 600 °C. Which was stem from the bioactive glass content in the SS-BG films. Since these particles was not affected from heat at those temperatures, they showed very limited weight losses.

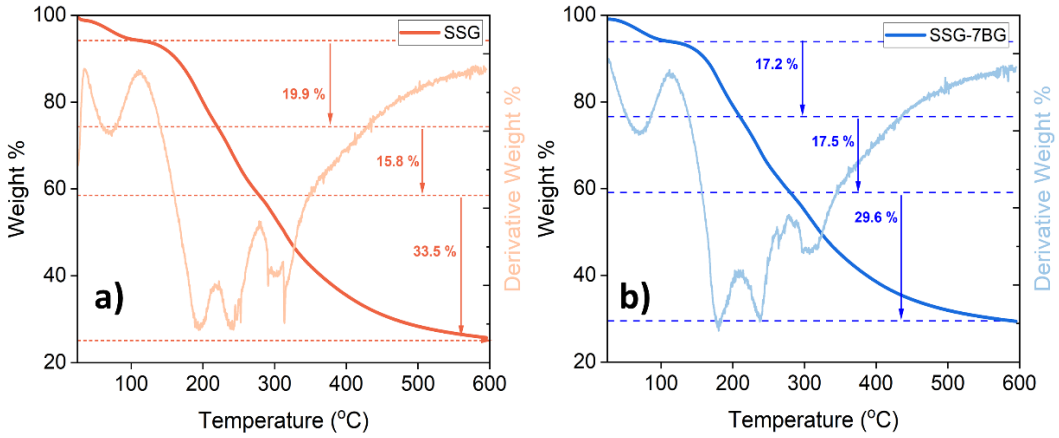

Figure 4.22 TGA curves and derivatives of the TGA curves of a) SSG and b) SSG-7BG samples.

SEM images of SSG-BGD samples were also investigated after 72 hours degradation in PBS (Figure 4.23a,b). SSG-BGD films showed brittle fracture behavior after degradation which was due to the loss of plasticizer. In their cross-sections, it was observed that after degradation BG particles near the surface of the fracture plane were detached from the film and left spherical holes (Figure 4.23b). The size of these voids were matched with the particle size of bioactive glasses, thus it can be deduced that they were the belong to BG phase.

Since it was seen that secondary reinforcing phase left the system during degradation, it is important to know that whether there were any secondary phase left in the system. EDS results after degradation (Figure 4.23c) indicates that elements came from bioactive glass phase like Ca and Si still present in the films after degradation. Therefore, it can be said that only the reinforcements near the film surfaces were detached either during glycerol difusion or due to mechanical forces during fracture.

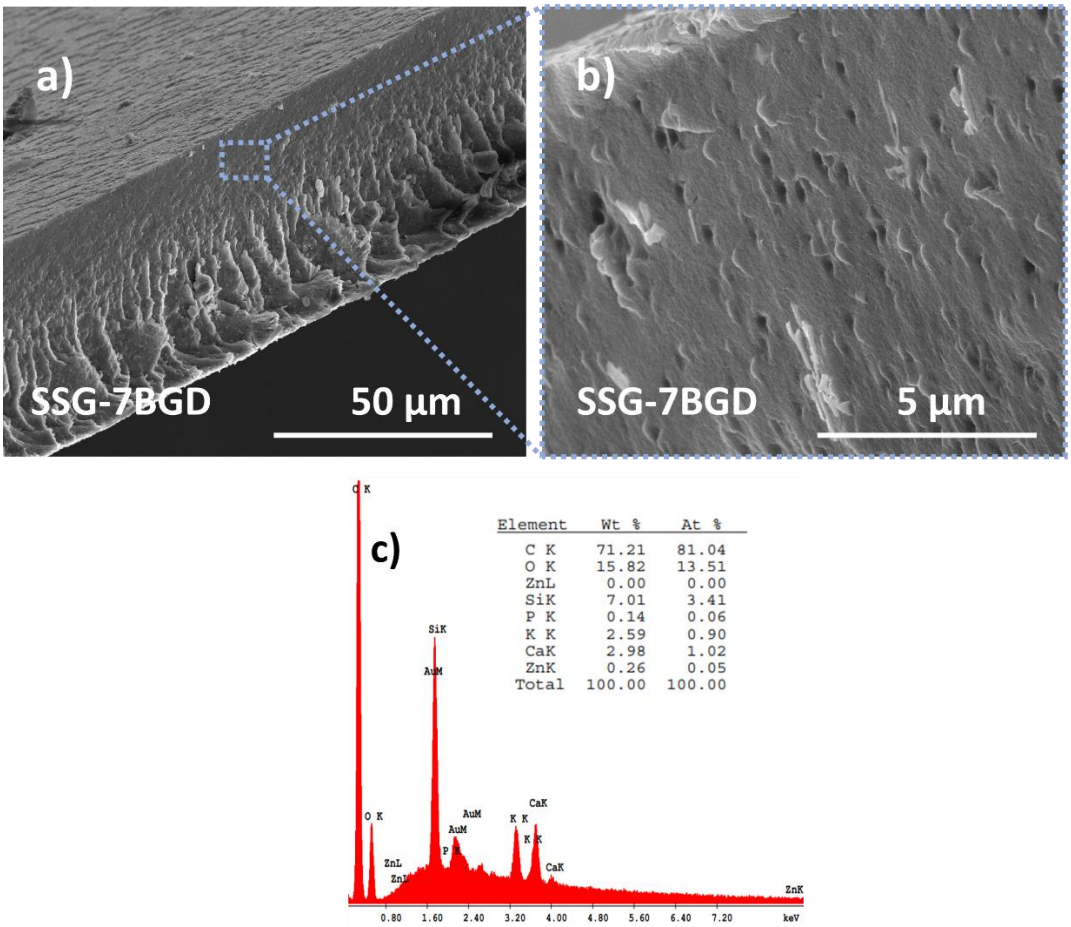

Figure 4.23 (a-b) Cross-sectional SEM images and c) EDS spectra of SSG-7BGD samples after soaking in 1xPBS for 72 h.

Swelling behavior of the films were directly related to their water retention ability which is crucial for wound dressing applications. This characteristics could be affected by the addition of BG particles. However, comparing the % swelling raitos (Figure 4.24a), SSG and SSG-3BG samples did not show any statistical difference in each time points. While SSG-7BG samples were the lowest water retention ability, SSG-3BG ones showed the highest % swelling up to 105%. Nevertheless, all samples has a average swelling ratio of 90-100 %. Which means they can retain water more than their initial weigths in the wet form. % swelling showed a

decreasing trend with increasing BG content. Depending on this result, it can be said that BG particles could physically compacts the films and slight decrease was observed in water retention ability.

Due to its biodegradability, mass loss was another important parameter for these sericin based films. Effect of %BG in SSG-BG films was shown in Figure 4.24b It was shown that all SSG-BG films lost nearly 35% their initial weights in the early stage of degradation. This could be the effect of glycerol since XRD and FTIR results showed that glycerol left the films during degradation. Thus, it can be said that glycerol seperation nearly completes during the first hour of degradation and no significant mass loss were observed after that.

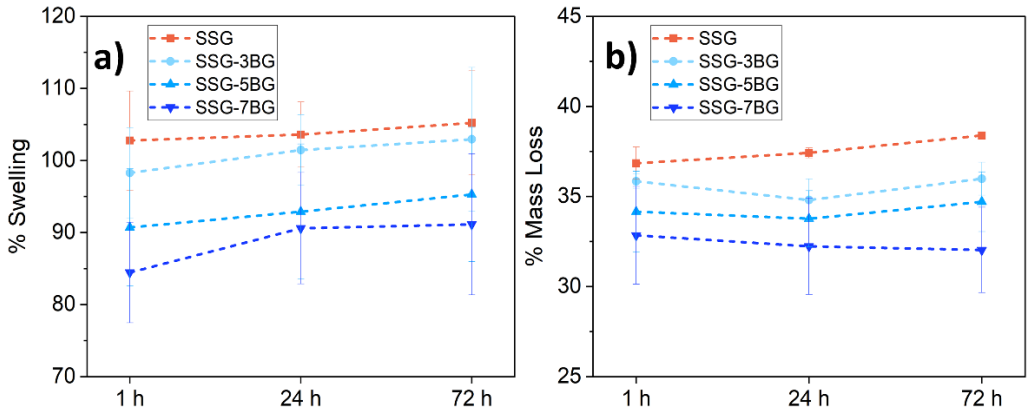

Figure 4.24 a) % swelling and b) % mass loss of SSG and SSG-BG samples in 1xPBS up to 72 h.

No significant changes in X-ray diffraction patterns of SSG-BG films were observed with respect to the changing BG concentration from 3 to 7 %. They all showed a major peak at 2Θ=21° and a small bump at 2Θ=14°. Similar to SSG-GO samples, that major peak can be caused by the addition of glycerol. To see the effect of degradation, comparing XRD patterns of SS, SSG, SSG-7BG and SSG-

7BGD films in Figure 4.25 it was observed that, after degradation peak intensity at 2Θ=21° reduced while 2Θ=14° one, which is also the major peak of sole sericin, becomes prominent. Since the peak at 2Θ=21°, which was also came from the silica hump of BG, was not vanished completely it can be said that after degradation, glycerol mostly left the system while sericin and BG remained. Yet, BG particles were not showed any effect on XRD spectra.

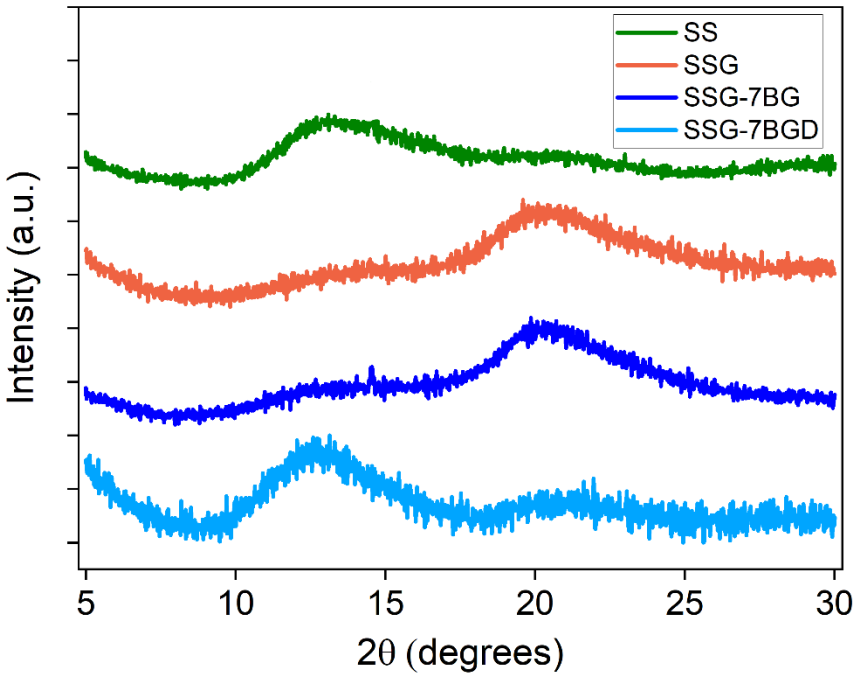

Figure 4.25 XRD spectra of SS, SSG, SSG-7BG and SSG-7BGD samples.

SSG-BG films with all concentrations showed same glycerol peaks at 1108 (C-O) and 995 (C=C) cm^{-1}. Also, similar to previous SSG and SSG-GO samples, these peaks were diminished after degradation due to glycerol seperation (Figure 4.26). However, in SSG-BG samples, two extra peaks were observed in the FTIR curves, especially became more clear after degradaion since they coincide with the glycerol peaks, at 1062 and 440 cm^{-1} which were corresponded to asymmetric P-O bond and Si-O-Si bands of BG particles (Figure 4.17d) with small shifts. This phenomenon

further approves the presence of BG in the films after degradation. In addition, it can be said that BG particles were not altered the chemical structure of sercin.

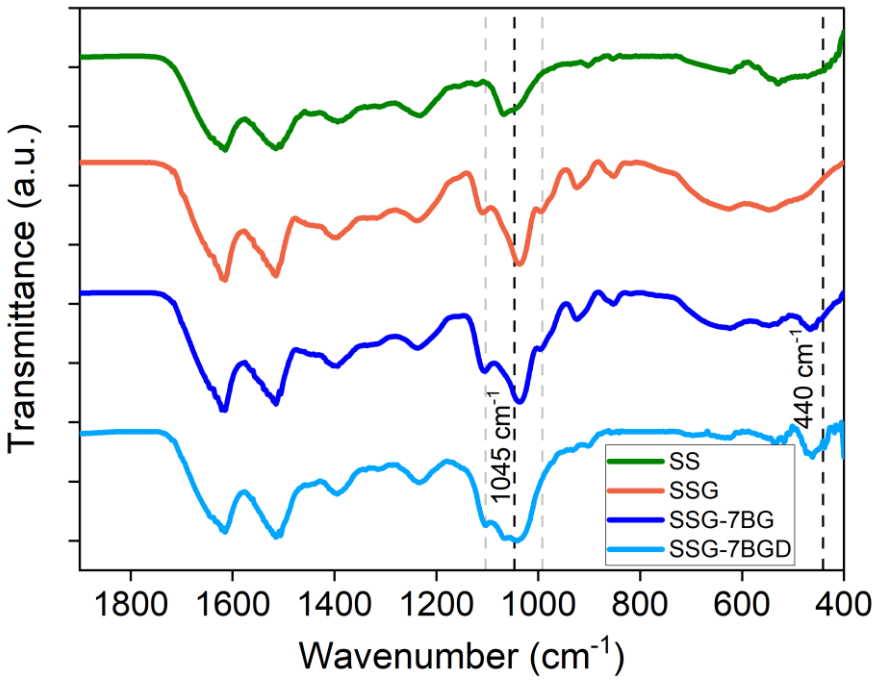

Figure 4.26 FTIR spectra of SS, SSG, SSG-7BG and SSG-7BGD samples.

Toxicity of SS-GO films were evaluated by using MTT assay. L929 fibroblast cells were cultured with 0.01g/ml extracts of all samples in DMEM up to 7 days. Indirect contact results (Figure 4.27) demonstrated that SSG-BG films show no toxicity on fibroblast cells which can protect viability up to 7 days. In fact, there could be a trend of increasing O.D. values with increasing BG concentration especially after 3 days of culture. Yet, no statictically important difference was observed in the adhesion and proliferation patterns for all three groups and the control group which was seeded on a treated polystryrene (TCP) surface and cultured with regular DMEM medium.

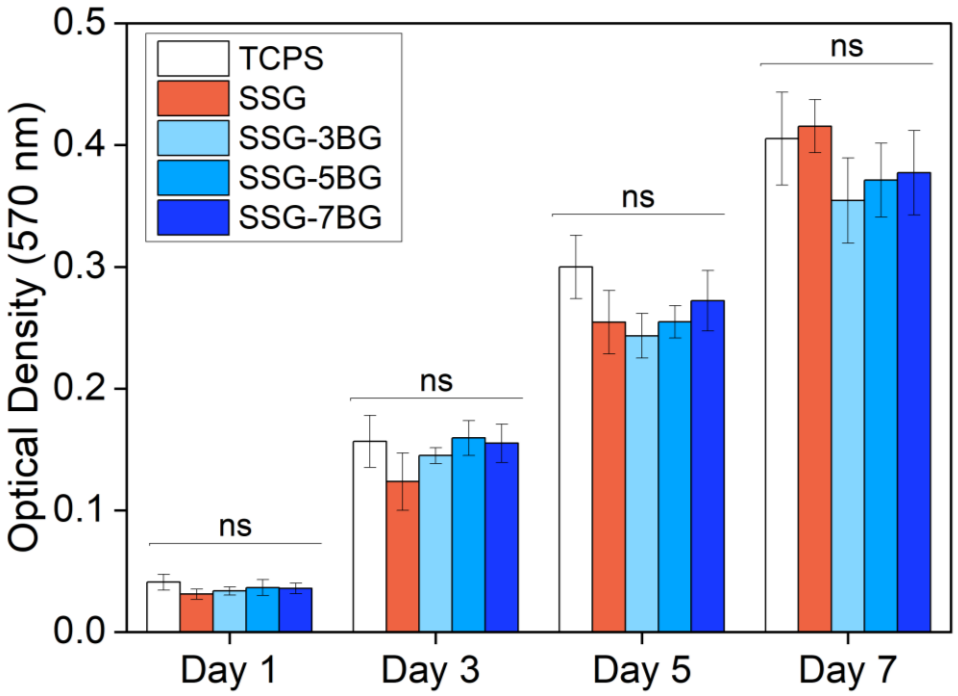

Figure 4.27 Viability of L929 fibroblasts up to 7 days *in vitro*. Values are mean ± SD (n=3), ns: non-significant.

To evaluate the antibacteral activity of SS-BG films, 2 bacteria groups namely *s. aureus* and *e. coli* were used as the gram positive and negative strains respectively in the experiments. 0.01g/ml extracts of three different composition of BG (SSG-3BG, SSG-5BG and SSG-7BG) samples were prepared in 0.3% TSB media. After culturing with both the gram positive and negative bacteria, resulted colony numbers were counted on agar plates after serial dilutions.

All samples show an antibacterial activity against *s. aureus.* SSG-3BG samples decreases the CFU amount up to 44%, while SS-5BG show a significant decrease of 56% with respect to control group SSG. In addition, SSG-7BG samples reduces the colony forming unit count up to 42% (Figure 4.28). Slight pH increase as well as the positively charged Zn ions could be responsible for this antibacterial effect since it can easily interact with the negatively charged bacterial wall and disrupt its

integrity [47]. Also, since small portion of BG particles were detached during degradation (Figure 4.17), direct contact inhibition could be a factor [42], [68].

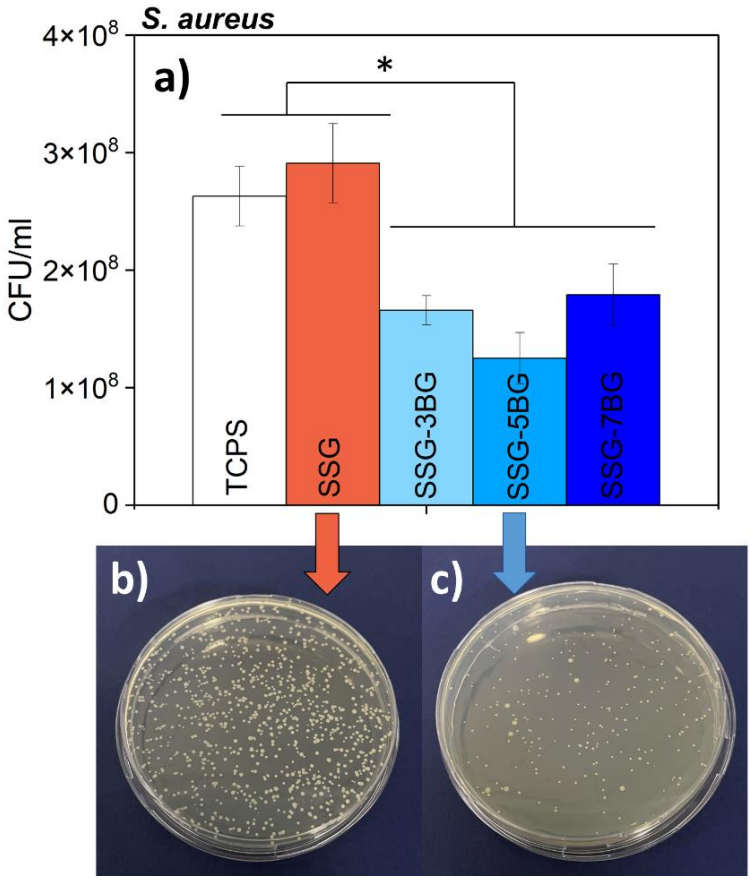

Figure 4.28 a) *S. aureus* colony counts for SS-BG films and (b-c) photographs of agar plates for b) SSG and c) SSG-5BG samples at 24 h of culture. Values are mean ± SD (n=3), *p< 0.05.

For the gram negative *e. coli*. however (Figure 4.29), 3% BG show no antibacterial effect. In fact, although there is a relative decrease in the colony counts 5% BG samples cannot show significant decrease in the CFU amount. Yet, after 5%, SSG-7BG samples show a statistial decrease in the colony count up to 27%. Therefore, it can be said that BG particles became effective against gram negative *e. coli*. when

their concentrations were higher than 5%. Which indicates that BG particles show a composition dependent antibacterial behaviour. Therefore, increasing the BG concentration could be more effective in the future works.

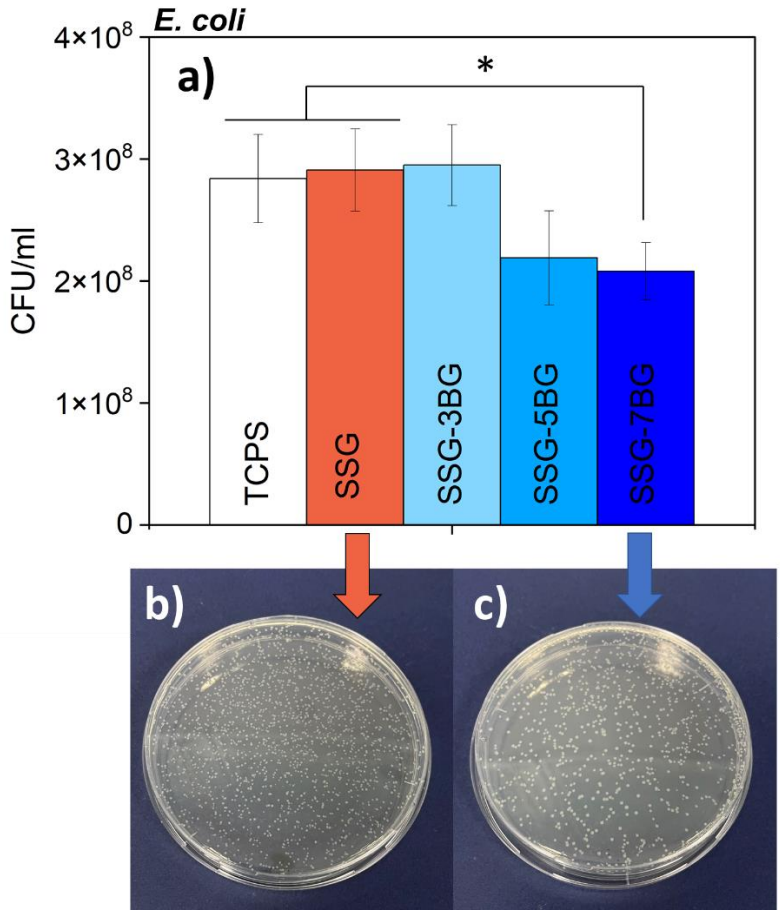

Figure 4.29 a) *E. coli* colony counts for SS-BG films and (b-c) photographs of agar plates for b) SSG and c) SSG-7BG samples at 24 h of culture. Values are mean ± SD (n=3), *$p< 0.05$.

CHAPTER 5

CONCLUSIONS

Due to having versatile properties, silk sericin became an important candidate for biomedical applications especially in the last decade. Selection of reinforging agents in this thesis demonstrated that various characteristics of sericin, including mechanical and biological properties, can be improved for temporary wound dressing applications.

In this study, sericin was successfully extracted using high temperature and pressure method. Glycerol was used as plasticizer to provide the desired flexibility to sericin films without any phase seperation. Although XRD and FTIR results showed that glycerol diffused out the system at the early stages of degradation, processing and preparation got much easier upon the use of glycerol. Furthermore, with the addition of GO and BG as reinforcements up to 1 and 7% respectively, flexible sericin based composite films were fabricated. Owing to the effective dispersion of these secondary phase reinforcements,which was confirmed in the SEM images, films with enhanced Young's modulus values up to 19.3±1.9 MPa for 1% GO and 22.4±0.6 MPa for 7% BG were obtained. Moreover, films showed 85 to 105% swelling in 1xPBS, which indicated water retention ability of the fabricated films. Biological properties of the sericin based films were also evaluated *in vitro*. Toxicity of the films were investigated by MTT assay and the results showed that L929 fibroblast cells remained viable with successful proliferation up to 7 days of culture. Antibacterial activity of these films was studied against gram-positive *S. aureus* and gram-negative *E. coli* strains. Both sample groups showed a reduction in the colony counts for both bacteria strains.

Due to having smaller size, lower amounts of GO showed the similar effect as higher concentrations of BG for both mechanical and antibacterial properties. Yet,

ion incorporation provides a wide range of adjustable properties to the resulted films. Thus, if the antibacterial activity is concerned GO could be preferred reinforcement phase whereas SS/BG composites can be useful where the cell interaction is important.

As a result, these findings demonstrated that besides its intrinsic properties with the adequate plasticizers and antibacterial agents, sericin could potentially be utilized as an alternative wound dressing material. Moreover, due to the adjustable properties and protein-based nature of the sericin, its application areas could be further enhanced in biomedical area.

CHAPTER 6

FUTURE WORK

Although this work showed that sericin based composite films can be considered as alternative wound dressing materials, several aspects can further be investigated in future studies:

- Gas permeability tests can be conducted using the sericin based composite films.
- Angiogenic properties of the silk sericin films can be tested *in vitro.*
- More adequate equipment can be used to disperse the secondasy phae more effectively.
- Higher amounts of reinforcements can be combined with sericin
- Swelling and degradation behavior of the films can be tested at earlier and later time points.
- Finally, *in vivo* performance of sericin based composite films can be assessed.

REFERENCES

[1] L. Lamboni, M. Gauthier, G. Yang, and Q. Wang, “Silk sericin: A versatile material for tissue engineering and drug delivery,” *Biotechnol Adv*, vol. 33, no. 8, pp. 1855–1867, Dec. 2015, doi: 10.1016/J.BIOTECHADV.2015.10.014.

[2] D. Gupta, A. Agrawal, H. Chaudhary, M. Gulrajani, and C. Gupta, “Cleaner process for extraction of sericin using infrared,” *J Clean Prod*, vol. 52, pp. 488–494, Aug. 2013, doi: 10.1016/J.JCLEPRO.2013.03.016.

[3] Z. Jiao *et al.*, “In Vivo Characterizations of the Immune Properties of Sericin: An Ancient Material with Emerging Value in Biomedical Applications,” *Macromol Biosci*, vol. 17, no. 12, p. 1700229, Dec. 2017, doi: 10.1002/MABI.201700229.

[4] P. Aramwit and A. Sangcakul, “The Effects of Sericin Cream on Wound Healing in Rats,” *Biosci. Biotechnol. Biochem*, vol. 71, no. 10, pp. 2473–2477, 2007, doi: 10.1271/bbb.70243.

[5] T. Siritientong, A. Angspatt, J. Ratanavaraporn, and P. Aramwit, “Clinical Potential of a Silk Sericin-Releasing Bioactive Wound Dressing for the Treatment of Split-Thickness Skin Graft Donor Sites”, doi: 10.1007/s11095-013-1136-y.

[6] S. C. Kundu, B. C. Dash, R. Dash, and D. L. Kaplan, “Natural protective glue protein, sericin bioengineered by silkworms: Potential for biomedical and biotechnological applications,” *Progress in Polymer Science (Oxford)*, vol. 33, no. 10, pp. 998–1012, Oct. 2008, doi: 10.1016/J.PROGPOLYMSCI.2008.08.002.

[7] J. Liu *et al.*, “Silk sericin-based materials for biomedical applications,” *Biomaterials*, vol. 287, Aug. 2022, doi: 10.1016/J.BIOMATERIALS.2022.121638.

[8] P. Aramwit, T. Siritientong, and T. Srichana, “Potential applications of silk sericin, a natural protein from textile industry by-products Silk protein and its use”, *Waste Management & Research*, vol. 30, no. 3, doi: 10.1177/0734242X11404733.

[9] V. H. Resh and R. T. Carde, *Encyclopedia of Insects*. Elsevier Inc., 2009. doi: 10.1016/B978-0-12-374144-8.X0001-X.

[10] P. Poza, J. Pérez-Rigueiro, M. Elices, and J. LLorca, “Fractographic analysis of silkworm and spider silk,” *Eng Fract Mech*, vol. 69, no. 9, pp. 1035–1048, Jun. 2002, doi: 10.1016/S0013-7944(01)00120-5.

[11] T. T. Cao and Y. Q. Zhang, “Processing and characterization of silk sericin from Bombyx mori and its application in biomaterials and biomedicines,” *Materials Science and Engineering C*, vol. 61, pp. 940–952, Apr. 2016, doi: 10.1016/J.MSEC.2015.12.082.

[12] J. Saha, M. H. Ibrahim Mondal, M. Rezaul Karim Sheikh, M. Ahsan Habib, and I. H. Mondal, “Extraction, Structural and Functional Properties of Silk Sericin Biopolymer from Bombyx mori Silk Cocoon Waste,” 2019, doi: 10.4172/2165-8064.1000390.

[13] W. Qiu, A. Patil, F. Hu and X. Y. Liu, “Hierarchical Structure of Silk Materials Versus Mechanical Performance and Mesoscopic Engineering Principles,” *Small*, vol. 15, no. 51, p. 1903948, Dec. 2019, doi: 10.1002/SMLL.201903948.

[14] A. S. Silva, E. C. Costa, S. Reis, C. Spencer, R. C. Calhelda *et al.*, “Silk Sericin: A Promising Sustainable Biomaterial for Biomedical and Pharmaceutical Applications,” *Polymers 2022, Vol. 14, Page 4931*, vol. 14, no. 22, p. 4931, Nov. 2022, doi: 10.3390/POLYM14224931.

[15] P. Aramwit, S. Kanokpanont, T. Nakpheng, and T. Srichana, “The Effect of Sericin from Various Extraction Methods on Cell Viability and Collagen Production,” *Int J Mol Sci*, vol. 11, no. 5, p. 2200, 2010, doi: 10.3390/IJMS11052200.

[16] C. J. Park, J. Ryoo, C. S. Ki, J. W. Kim, I. S. Kim *et al.*, “Effect of molecular weight on the structure and mechanical properties of silk sericin gel, film, and sponge,” *Int J Biol Macromol*, vol. 119, pp. 821–832, Nov. 2018, doi: 10.1016/J.IJBIOMAC.2018.08.006.

[17] Y. J. Yoo and I. C. Um, “Effect of Extraction Time on the Rheological Properties of Sericin Solutions and Gels,” *Int J Indust Entomol*, vol. 27, no. 1, pp. 180–184, Sep. 2013, doi: 10.7852/IJIE.2013.27.1.180.

[18] H. J. Jin and D. L. Kaplan, “Mechanism of silk processing in insects and spiders,” *Nature*, vol. 424, no. 6952, pp. 1057–1061, Aug. 2003, doi: 10.1038/NATURE01809.

[19] P. Cebe, B. P. Partlow, D. L. Kaplan, A. Wurm, E. Zhuravlev, and C. Schick, “Silk I and Silk II studied by fast scanning calorimetry,” *Acta Biomater*, vol. 55, pp. 323–332, Jun. 2017, doi: 10.1016/J.ACTBIO.2017.04.001.

[20] M. Elahi, S. Ali, H. M. Tahir, R. Mushtaq and M. F. Bhatti, “Sericin and fibroin nanoparticles—natural product for cancer therapy: a comprehensive review,” *International Journal of Polymeric Materials and Polymeric Biomaterials*, vol. 70, no. 4, pp. 256–269, Mar. 2021, doi: 10.1080/00914037.2019.1706515.

[21] A. Z. Siavashani, J. Mohammadi, M. Rottmar, B. Senturk, J. Nourmohammadi *et al.*, “Silk fibroin/sericin 3D sponges: The effect of sericin on structural and biological properties of fibroin,” *Int J Biol Macromol*, vol. 153, pp. 317–326, Jun. 2020, doi: 10.1016/J.IJBIOMAC.2020.02.316.

[22] B. O. Ode Boni, B. M. Bakadia, A. R. Osi, Z. Shi, H. Chen *et al.*, "Immune Response to Silk Sericin–Fibroin Composites: Potential Immunogenic Elements and Alternatives for Immunomodulation," *Macromol Biosci*, vol. 22, no. 1, Jan. 2022, doi: 10.1002/MABI.202100292.

[23] M. He, H. Hu, P. Wang, H. Fu, J. Yuan *et al.*, "Preparation of a bio-composite of sericin-g-PMMA via HRP-mediated graft copolymerization," *Int J Biol Macromol*, vol. 117, pp. 323–330, Oct. 2018, doi: 10.1016/J.IJBIOMAC.2018.05.190.

[24] L. Zhang, W. Yang, K. Tao, Y. Song, H. Xie *et al.*, "Sustained local release of NGF from a chitosan-sericin composite scaffold for treating chronic nerve compression," *ACS Appl Mater Interfaces*, vol. 9, no. 4, pp. 3432–3444, Feb. 2017, doi: 10.1021/ACSAMI.6B14691/ASSET/IMAGES/LARGE/AM-2016-14691H_0006.JPEG.

[25] P. Aramwit, T. Siritientong, S. Kanokpanont, and T. Srichana, "Formulation and characterization of silk sericin–PVA scaffold crosslinked with genipin," *Int J Biol Macromol*, vol. 47, no. 5, pp. 668–675, Dec. 2010, doi: 10.1016/J.IJBIOMAC.2010.08.015.

[26] G. Tao, Y. Wang, R. Cai, H. Chang, K. Song *et al.*, "Design and performance of sericin/poly(vinyl alcohol) hydrogel as a drug delivery carrier for potential wound dressing application," *Mater Sci Eng C Mater Biol Appl*, vol. 101, pp. 341–351, Aug. 2019, doi: 10.1016/J.MSEC.2019.03.111.

[27] H. Zhang, L. Deng, M. Yang, S. Min, L. Yang, and L. Zhu, "Enhancing Effect of Glycerol on the Tensile Properties of Bombyx mori Cocoon Sericin Films," *OPEN ACCESS Int. J. Mol. Sci*, vol. 12, p. 12, 2011, doi: 10.3390/ijms12053170.

[28] H. Yun, M. K. Kim, H. W. Kwak, J. Y. Lee, M. H. Kim, and K. H. Lee, "The role of glycerol and water in flexible silk sericin film," *Int J Biol Macromol*, vol. 82, pp. 945–951, Jan. 2016, doi: 10.1016/J.IJBIOMAC.2015.11.016.

[29] H. Yun, M. K. Kim, H. W. Kwak, J. Y. Lee *et al.*, "Preparation and characterization of silk sericin/glycerol/graphene oxide nanocomposite film," *Fibers and Polymers*, vol. 14, no. 12, pp. 2111–2116, Dec. 2013, doi: 10.1007/S12221-013-2111-2/METRICS.

[30] J. W. Fluhr, R. Darlenski, and C. Surber, "Glycerol and the skin: Holistic approach to its origin and functions," *British Journal of Dermatology*, vol. 159, no. 1. pp. 23–34, Jul. 2008. doi: 10.1111/j.1365-2133.2008.08643.x.

[31] Z. Ghlissi, N. Sayari, R. Kallel, A. Bougatef, and Z. Sahnoun, "Antioxidant, antibacterial, anti-inflammatory and wound healing effects of Artemisia campestris aqueous extract in rat," *Biomedicine and Pharmacotherapy*, vol. 84, pp. 115–122, Dec. 2016, doi: 10.1016/j.biopha.2016.09.018.

[32] S. Nayak, T. Dey, D. Naskar, and S. C. Kundu, "The promotion of osseointegration of titanium surfaces by coating with silk protein sericin," *Biomaterials*, vol. 34, no. 12, pp. 2855–2864, Apr. 2013, doi: 10.1016/J.BIOMATERIALS.2013.01.019.

[33] S. Liu, T. H. Zeng, M. Hofmann, E. Burcombe, J. Wei *et al.*, "Antibacterial activity of graphite, graphite oxide, graphene oxide, and reduced graphene oxide: Membrane and oxidative stress," *ACS Nano*, vol. 5, no. 9, pp. 6971–6980, Sep. 2011, doi: 10.1021/nn202451x.

[34] M. Yousefi, M. Dadashpour, M. Hejazi, M. Hasanzadeh, B. Behnam *et al.*, "Anti-bacterial activity of graphene oxide as a new weapon nanomaterial to combat multidrug-resistance bacteria," *Materials Science and Engineering C*, vol. 74. Elsevier Ltd, pp. 568–581, May 01, 2017. doi: 10.1016/j.msec.2016.12.125.

[35] K. Krishnamoorthy, N. Umasuthan, R. Mohan, J. Lee, and S. J. Kim, "Antibacterial activity of graphene oxide nanosheets," *Sci Adv Mater*, vol. 4, no. 11, pp. 1111–1117, Nov. 2012, doi: 10.1166/SAM.2012.1402.

[36] O. Akhavan and E. Ghaderi, "Toxicity of graphene and graphene oxide nanowalls against bacteria," *ACS Nano*, vol. 4, no. 10, pp. 5731–5736, Oct. 2010, doi: 10.1021/NN101390X/ASSET/IMAGES/LARGE/NN-2010-01390X_0005.JPEG.

[37] S. Gurunathan, J. W. Han, A. Abdal Dayem, V. Eppakayala, and J. H. Kim, "Oxidative stress-mediated antibacterial activity of graphene oxide and reduced graphene oxide in Pseudomonas aeruginosa," *Int J Nanomedicine*, vol. 7, p. 5901, 2012, doi: 10.2147/IJN.S37397.

[38] O. Akhavan and E. Ghaderi, "Toxicity of graphene and graphene oxide nanowalls against bacteria," *ACS Nano*, vol. 4, no. 10, pp. 5731–5736, Oct. 2010, doi: 10.1021/nn101390x.

[39] C. Qi, Y. Deng, L. Xu, C. Yang, Y. Zhu *et al.*, "A sericin/ graphene oxide composite scaffold as a biomimetic extracellular matrix for structural and functional repair of calvarial bone," *Theranostics*, vol. 10, no. 2, pp. 741–756, 2020, doi: 10.7150/thno.39502.

[40] B. Jayavardhini, Y. R. Pravin, C. Kumar, R. Murugesan, and S. W. Vedakumari, "Graphene oxide impregnated sericin/collagen scaffolds – Fabrication and characterization," *Mater Lett*, vol. 307, Jan. 2022, doi: 10.1016/j.matlet.2021.131060.

[41] M. Zhang, D. Wang, N. Ji, S. Lee, G. Wang *et al.*, "Bioinspired design of sericin/chitosan/ag@mof/go hydrogels for efficiently combating resistant bacteria, rapid hemostasis, and wound healing," *Polymers (Basel)*, vol. 13, no. 16, Aug. 2021, doi: 10.3390/polym13162812.

[42] I. Cacciotti, "Bivalent cationic ions doped bioactive glasses: the influence of magnesium, zinc, strontium and copper on the physical and biological

properties," *J Mater Sci*, vol. 52, no. 15, pp. 8812–8831, Aug. 2017, doi: 10.1007/s10853-017-1010-0.

[43] S. M. Rabiee, N. Nazparvar, M. Azizian, D. Vashaee, and L. Tayebi, "Effect of ion substitution on properties of bioactive glasses: A review," *Ceramics International*, vol. 41, no. 6. Elsevier Ltd, pp. 7241–7251, Jul. 01, 2015. doi: 10.1016/j.ceramint.2015.02.140.

[44] L. Mao, L. Xia, J. Chang, J. Liu, L. Jiang *et al.*, "The synergistic effects of Sr and Si bioactive ions on osteogenesis, osteoclastogenesis and angiogenesis for osteoporotic bone regeneration," *Acta Biomater*, vol. 61, pp. 217–232, Oct. 2017, doi: 10.1016/j.actbio.2017.08.015.

[45] F. Zhao, B. Lei, Z. Li, Y. Mo, R. Wang *et al.*, "Promoting in vivo early angiogenesis with sub-micrometer strontium-contained bioactive microspheres through modulating macrophage phenotypes," *Biomaterials*, vol. 178, pp. 36–47, Sep. 2018, doi: 10.1016/j.biomaterials.2018.06.004.

[46] S. Kargozar, M. Montazerian, S. Hamzehlou, H. W. Kim, and F. Baino, "Mesoporous bioactive glasses: Promising platforms for antibacterial strategies," *Acta Biomaterialia*, vol. 81. Acta Materialia Inc, pp. 1–19, Nov. 01, 2018. doi: 10.1016/j.actbio.2018.09.052.

[47] J. Pasquet, Y. Chevalier, J. Pelletier, E. Couval, D. Bouvier, and M. A. Bolzinger, "The contribution of zinc ions to the antimicrobial activity of zinc oxide," *Colloids Surf A Physicochem Eng Asp*, vol. 457, no. 1, pp. 263–274, Sep. 2014, doi: 10.1016/j.colsurfa.2014.05.057.

[48] H. Zhu, N. Liu, X. Feng, and J. Chen, "Fabrication and characterization of silk fibroin/bioactive glass composite films," *Materials Science and Engineering: C*, vol. 32, no. 4, pp. 822–829, May 2012, doi: 10.1016/J.MSEC.2012.01.033.

[49] J. Boateng and O. Catanzano, "Advanced Therapeutic Dressings for Effective Wound Healing - A Review," *Journal of Pharmaceutical Sciences*,

vol. 104, no. 11. John Wiley and Sons Inc., pp. 3653–3680, Nov. 01, 2015. doi: 10.1002/jps.24610.

[50] Y. Liang, Y. Liang, H. Zhang, and B. Guo, “Antibacterial biomaterials for skin wound dressing,” *Asian Journal of Pharmaceutical Sciences*, vol. 17, no. 3. Shenyang Pharmaceutical University, pp. 353–384, May 01, 2022. doi: 10.1016/j.ajps.2022.01.001.

[51] E. Rezvani Ghomi, S. Khalili, S. Nouri Khorasani, R. Esmaeely Neisiany, and S. Ramakrishna, “Wound dressings: Current advances and future directions,” *Journal of Applied Polymer Science*, vol. 136, no. 27. John Wiley and Sons Inc., Jul. 15, 2019. doi: 10.1002/app.47738.

[52] S. Dhivya, V. V. Padma, and E. Santhini, “Wound dressings - A review,” *BioMedicine (Netherlands)*, vol. 5, no. 4. China Medical University, pp. 24–28, Dec. 01, 2015. doi: 10.7603/s40681-015-0022-9.

[53] G. Han and R. Ceilley, “Chronic Wound Healing: A Review of Current Management and Treatments,” *Advances in Therapy*, vol. 34, no. 3. Springer Healthcare, pp. 599–610, Mar. 01, 2017. doi: 10.1007/s12325-017-0478-y.

[54] M. Farokhi, F. Mottaghitalab, Y. Fatahi, A. Khademhosseini, and D. L. Kaplan, “Overview of Silk Fibroin Use in Wound Dressings,” *Trends in Biotechnology*, vol. 36, no. 9. Elsevier Ltd, pp. 907–922, Sep. 01, 2018. doi: 10.1016/j.tibtech.2018.04.004.

[55] M. Farahani and A. Shafiee, “Wound Healing: From Passive to Smart Dressings,” *Advanced Healthcare Materials*, vol. 10, no. 16. John Wiley and Sons Inc, Aug. 01, 2021. doi: 10.1002/adhm.202100477.

[56] Q. Zeng, X. Qi, G. Shi, M. Zhang, and H. Haick, “Wound Dressing: From Nanomaterials to Diagnostic Dressings and Healing Evaluations,” *ACS Nano*, vol. 16, no. 2. American Chemical Society, pp. 1708–1733, Feb. 22, 2022. doi: 10.1021/acsnano.1c08411.

[57] S. Gilotra, D. Chouhan, N. Bhardwaj, S. K. Nandi, and B. B. Mandal, "Potential of silk sericin based nanofibrous mats for wound dressing applications," *Materials Science and Engineering C*, vol. 90, pp. 420–432, Sep. 2018, doi: 10.1016/J.MSEC.2018.04.077.

[58] D. C. Marcano, D. V. Kosynkin, J. M. Berlin, A. Sinitskii, Z. Sun *et al.*, "Improved synthesis of graphene oxide," *ACS Nano*, vol. 4, no. 8, pp. 4806–4814, Aug. 2010, doi: 10.1021/nn1006368.

[59] V. Vagenende, M. G. S. Yap, and B. L. Trout, "Mechanisms of protein stabilization and prevention of protein aggregation by glycerol," *Biochemistry*, vol. 48, no. 46, pp. 11084–11096, Nov. 2009, doi: 10.1021/bi900649t.

[60] H. Teramoto, A. Kakazu, K. Yamauchi, and T. Asakura, "Role of hydroxyl side chains in Bombyx mori silk sericin in stabilizing its solid structure," *Macromolecules*, vol. 40, no. 5, pp. 1562–1569, Mar. 2007, doi: 10.1021/ma062604e.

[61] "Beauchamp Spectroscopy Tables"

[62] D. C. Marcano *et al.*, "Improved synthesis of graphene oxide," *ACS Nano*, vol. 4, no. 8, pp. 4806–4814, Aug. 2010, doi: 10.1021/nn1006368.

[63] S. Kellici, J. Acord, J. Ball, H. S. Reehal, D. Morgan, and B. Saha, "A single rapid route for the synthesis of reduced graphene oxide with antibacterial activities," *RSC Adv*, vol. 4, no. 29, pp. 14858–14861, 2014, doi: 10.1039/c3ra47573e.

[64] J. Du and H. M. Cheng, "The Fabrication, Properties, and Uses of Graphene/Polymer Composites," *Macromol Chem Phys*, vol. 213, no. 10–11, pp. 1060–1077, Jun. 2012, doi: 10.1002/MACP.201200029.

[65] A. Abdulkhani, M. Daliri Sousefi, A. Ashori, and G. Ebrahimi, "Preparation and characterization of sodium carboxymethyl cellulose/silk

fibroin/graphene oxide nanocomposite films," *Polym Test*, vol. 52, pp. 218–224, Jul. 2016, doi: 10.1016/j.polymertesting.2016.03.020.

[66] Y. Yuan *et al.*, "Simple fabrication of sericin/graphene nanocomposites for application in articular cartilage repair in knee joints in nursing care," *Applied Nanoscience (Switzerland)*, vol. 10, no. 3, pp. 695–702, Mar. 2020, doi: 10.1007/s13204-019-01150-x.

[67] A. Kalra, A. Lowe, and A. al Jumaily, "An Overview of Factors Affecting the Skin's Young's Modulus," 2016, doi: 10.4172/2329-8847.1000156.

[68] R. Sergi, D. Bellucci, and V. Cannillo, "A review of bioactive glass/natural polymer composites: State of the art," *Materials*, vol. 13, no. 23. MDPI AG, pp. 1–38, Dec. 01, 2020. doi: 10.3390/ma13235560.